UNIVERSITAT DE BARCELONA

Final Degree Project

Biomedical Engineering Degree

"Development of microchannels of tunable stiffness for the study of migration of T-cells"

Barcelona, 6th of June 2023

Author: Clàudia Araujo Albiol
Director/s: Jordi Comelles Pujadas
Tutor: Jordi Comelles Pujadas

Abstract

Cell migration plays a crucial role in various physiological and pathological processes, including immune response and cancer metastasis. The complex interplay of the cancer cells with the microenvironment and the immune cell recruitment has emerged as a critical aspect in the progression of colorectal cancer. Cytotoxic T lymphocytes infiltrate the tumour microenvironment to exert anti-tumour immunity. To get to the tumour stroma, cells have to extravasate the vascular endothelial barrier in a process called transendothelial migration. We herein develop a microfluidic device capable of investigating the migration of T cells within an environment that closely mimics *In vivo* tissue characteristics. We have developed different protocols to fabricate microchannels of two different materials, polydimethylsiloxane, and polyacrylamide. Photolithography and novel microfabrication techniques have been employed to acquire confined microchannels. The microchannels successfully recreated key aspects of *In vivo* environment, enabling precise control of size and confinement. We have studied and confirmed the advantages of using hydrogels in microfluidics and their tuneable mechanical properties have been proved. Finally, the PDMS microfluidic chip has been tested with Jurkat cells and we have confirmed the suitability of the device for studying T cell migration profiles.

Keywords: *Microfluidics / microchannels / hydrogels / stiffness / cell migration / confinement*

Acknowledgements

First of all, I would like to express my sincere gratitude to my director Jordi Comelles, for his guidance, teaching, and support through the whole project.

I would also like to express my gratitude to Dr Elena Martínez for giving me the chance to do this project in her group.

Lastly, I would like to extend my gratitude to all the Biomimetic systems for cell engineering group members for their warm welcome, for making me feel like one more of the group and for helping me whenever I needed it.

List of Figures

List of Tables

Table of contents

1.INTRODUCITON

Colorectal cancer (CRC) was one of the three most common cancers diagnosed in men and women in 2021 [1]. Extensive research in recent years has focused on the relationship between the tumor microenvironment (TME) and the progression of colorectal cancer. There has been growing interest in the network of tumor cells, stromal cells, immune cells, blood vessel cells, and fibroblasts that comprise the TME to identify new therapeutic interventions. And some studies conclude that TME, as a result of the communication between these cells, may play a key role in tumor development, metastasis and its prognostics [2], [3].

The genetic and cellular alterations that characterize cancer make the immune system generate T-cell responses that can identify and eliminate cancerous cells. However, it is essential to recognize that the extermination of cancer by T cells represents just a single stage in the complex process known as the Cancer-Immunity Cycle, seen in Figure 1. [4] In the first steps an anticancer T cell response is generated. And then the trafficking of T cells to tumor starts. After being released into the bloodstream, T cells undergo a transendothelial migration (TEM), a process in which they traverse the endothelial barrier to infiltrate the tumor microenvironment and exert their anti-tumor activities. Therefore, understanding the mechanisms and dynamics of T-cell migration is of paramount importance in interpreting the immune response against colorectal cancer and exploring potential therapeutic interventions.

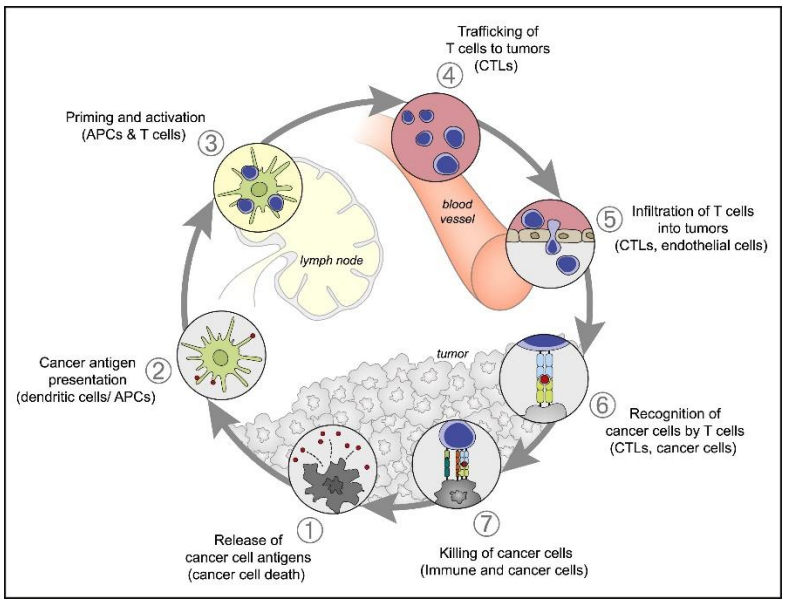

Figure 1: The Cancer-Immunity Cycle. [4]

Different migration assays and experimental methods have been developed and used for years. [5] However, traditional assays suffer from limitations that prevent their ability to replicate the in vivo conditions accurately. Cell migration has been studied in flat two-dimensional (2D) systems that do not reproduce many of the environment properties found in tissues, such as confinement and other mechanical properties like stiffness. Recent studies demonstrate that differences in the physical microenvironment (confined/unconfined) make cells adopt distinct signaling strategies to modulate cell migration [6]. This fact makes evident the necessity of overcoming current limitation in migration assays.

To overcome these limitations, there is a growing need to develop advanced microfluidic devices that can closely mimic the in vivo microenvironment experienced by T-cells during migration. These devices should incorporate key features such as confinement and mechanical properties, including the ability to reproduce the physiological stiffness of tissues. Hydrogels, for instance, offer an attractive option due to their tunable mechanical properties and the ability to achieve stiffness levels similar to those found in vivo. Three-dimensional (3D) hydrogels have demonstrated a notable capacity to mimic the extracellular environment. They are therefore suitable to studying cell migration in a physiologically relevant and more straightforward manner. Multiple synthetic and naturally derived hydrogels with heterogeneous characteristics and functional properties have been reported. [7] Being collagen gels the most famous, which aim at recapitulating the properties of the extracellular matrix (ECM) composition.

1.1. Aim and scope of the project

The current project aims at the development of a microfluidic platform to study Cytotoxic T lymphocytes (CTLs) migration through narrow channels of controllable size and mechanical properties. The device will be made of polyacrylamide (PA) hydrogels, which allow to reach physiological stiffness and, it will contain predesigned confined microchannels of different sizes and shapes. The device will be finally validated by testing the migration of an immune system cell line, Jurkat cells.

1.2. Objectives

As stated above, the main objective of the project is to obtain a microfluidic device with narrow channels of controllable size and stiffness. To achieve that, several objectives have been stablished:

I. Design the microfluidic platform and the microchannels we want to develop and implement them in a photomask to be used for further photolithography processes.
II. Obtain a master with the microchannels designs to be used as a mold for the final microfluidic chip.
III. Develop an effective protocol for the fabrication of the microchannels to acquire PDMS/PA replicas with the features imprinted on them.
IV. Assemble the obtained microchannels to a flat surface to get a confined microfluidic device.
V. Functionalize the walls of the microchannels with a proper coating with functionally active proteins.
VI. Perform cell migration experiments with the obtained device to validate its performance.

1.3. Methodology

The project has been done at the Institute of Bioengineering of Catalonia (IBEC), specifically at Biomimetic Systems for Cell Engineering group, which is headed by Dr. Elena Martínez Fraíz. The whole project has been developed from October 2022 to June 2023.

This has been a mainly experimental work, preceded by a first bibliographic research based in the different existent modalities, options and approaches, already running, of the microfluidic devices used in cell migration research. The layout of the experimental part of the project can be divided in

the following parts, which through the progress of the project have been modeled according to the obtained outcomes and the intermediate decisions that had to be made.

First of all, a designing task was performed to get the basis of the microfluidic device we wanted to obtain. Based on previous devices we designed different types of microchannels.

After that we started an optimization task for the fabrication of microchannels, concurrently working with two different materials polydimethylsiloxane (PDMS) and polyacrylamide (PA). While trying to get the best protocol for microchannels fabrication we started working, at the same time, with the bonding approach, which consisted of the arrangement of the fabricated microchannels to acquire the final microfluidic device. This step also involved a complex optimization process to find an efficient final microfluidic chip.

Finally, to test the obtained platforms, cell migration experiments were carried out to validate the developed devices and conclude if they fulfilled the preestablished objectives of the project.

The planning and follow up of the project have been managed by different planning tools based on the Work Breakdown Structure (WBS) and GANTT diagram, which are detailed in section 6. EXECUTION SCHEDULE.

2. BACKGROUND

In the following parts we will focus on the background of the project. The related devices and experimental approaches already developed in the field are going to be analyzed and we will also explain the framework in which the project is involved.

2.1. State of the art

In this section, the different approaches developed so far, that are used in cell migration studies, will be presented, and are illustrated in Figure 2. Then, we will focus on the microchannel devices currently used and their characteristics, and, finally, we will study the options already in use, in the field of hydrogels, which is what concerns us.

2.1.1. Cell migration studies

Several experimental methods have been described for assessing cell migration. Next, we list some of them from the most traditional ones to the recent developed strategies [8].

Traditional in vitro assays

- Boyden chambers (transwell systems): It consist of two cell culture chambers separated by a stiff, porous membrane. One way to measure migration is by counting the number of cells that move from one chamber to another through the membrane. [9] Although the system is simple to operate and has a high throughput, live cell imaging and gradient control are not supported. Adding a hydrogel, frequently a Matrigel, on top of the membrane to analyze invasion through a 3D matrix is a way to improve this test.
- Micropipette assay: Predefined chemokine solutions are dispensed using a controlled micropipette near cells on a 2D substrate [10], but the chemokine gradients that result are

temporary and challenging to quantify. However, it shows advantages over live imaging and local stimulation.

- Wound healing: They are used to evaluate collective cellular migration. Using a micropipette, a "wound" or an area free of cells is created, and cell motility is assessed by keeping track of how long it takes for the "wound" to be covered. It enables live imaging and high throughput analysis. But it is only applicable to two dimensional substrates. [11]

Microfluidic in vitro assays

Despite the wide variety of conventional assays, they fail to precisely control cells microenvironment and the stimuli they receive. Microfluidics allows us to consider many other parameters that have a key role in cell migration and are decisive for a variety of biological processes. For example, confinement, interstitial pressure, stiffness, constrictions, and other mechanical cues can be well reproduced in microfluidic assays [12].

Microfluidic devices are developed using microfabrication techniques and 3D matrices. They give us the chance to stablish different fluid streams in different channels, a large variety of designs can be obtained, and multiple cell types can be incorporated to even form what is nowadays known as Organ-on-Chip technology. Moreover, microscale systems can offer low sample consumption, rapid application of well-defined solutions, access to phenomena that are not accessible on the macroscopic scale, and significantly reduced analysis or experiment time [13].

Macroscale models

Macroscale models refer to hydrogel matrices such as collagen type I, Matrigel and synthetic materials that are used to investigate the effect of different extracellular matrix (ECM) properties on cell's tumor invasion. The assay consists of seeding cells uniformly inside the hydrogel and characterize their migration in real time monitoring or after a given period of time. Even so, they can not provide information at the microscale level like other assays such as microfluidics [8].

Micropatterned models

Micropatterned models aim to create patterned substrates to replicate the topography and architecture of in vivo environment. They can also include tunable constrictions and study, thus, the effect of physical and geometrical cues on cell migration. Although, these assays do not offer fluid flows and hence the application of chemical gradients. The fabrication of micropatterned models can be based in different microfabrication technologies, for example, soft lithography-based patterning. This technique uses elastomeric PDMS stamps with patterned relief features to generate microscale patterns [8], [14].

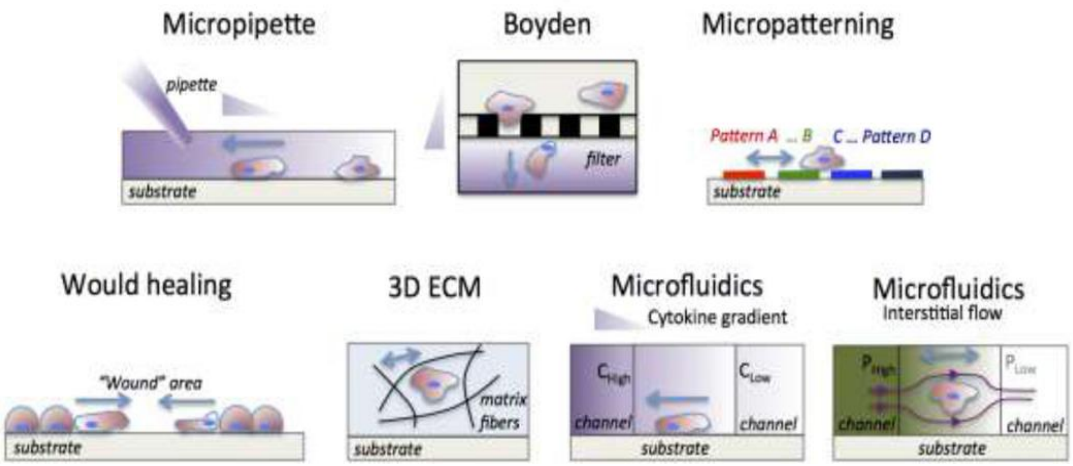

Figure 2: Different In vitro assays and experimental methods for investigating factors that influence cell migration. Adapted from [8].

2.1.2. Microchannel devices

From the different migration assays exposed, the one which offers more study possibilities and advantages in replicating in vivo conditions are microfluidic devices.

Till now, the most broadly used material in microfluidics has been polydimethylsiloxane (PDMS). The advantageous material properties and the simple fabrication methodologies that it offers have made it the gold standard for different microfluidic applications. It allows the formation of 3D fluid networks using a multilayer configuration and it is possible to optically access the migration area with a standard objective, allowing live imaging of the cells during their migration [12].

It is feasible to use various geometries, with increasing complexity. In cell migration assays microfluidic channels are designed generally based on the same strategies. The simplest geometry used to study cell migration and chemotaxis consists of an array of straight channels connecting two reservoirs. One of the reservoirs is used for cell seeding and the other to create a chemical gradient. This type of experiments allows to study the minimum channel cross-section that cells can afford, the effect of the chemoattractant on cell's velocity to cross the channels, and furthermore, the shape of the channels can be engineered to induce controlled spatial stimuli by designing channels that taper from smaller to higher widths. Examples of different geometries employed in PDMS devices are showed in Figure 3 [12].

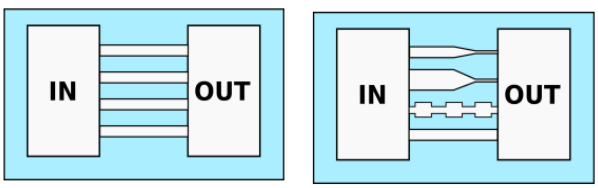

Figure 3: Different PDMS microchannel designs.

Figure 4 shows a real application where a PDMS chip is fabricated to study cell migration under confinement in one direction. PDMS channels were replicated from a channel mold. After resizing and making holes, the chip was bond on top of a glass dish to create confined microchannels. They successfully analyzed the cell migration profile of a large number of cells by imaging with phase contrast (10x) microscope [15].

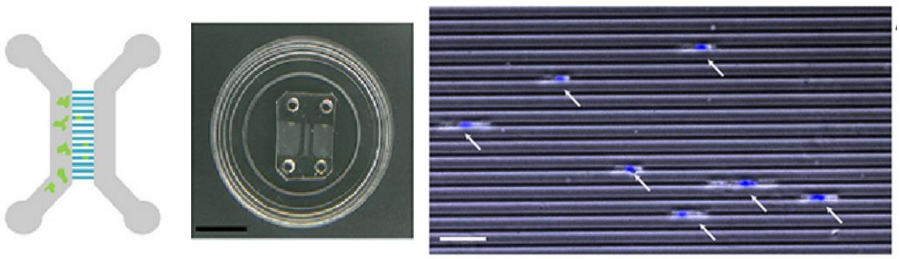

Figure 4: PDMS chip. From left to right, scheme of the chip, final chip assembled and microscope image of cells migrating through 5µm x 5µm microchannels. Scale bar of 50µm. Adapted from [15].

2.1.3. Hydrogel microchannels

While PDMS devices emulate size and confinement parameters *In vitro*, their channel walls are impermeable and have supraphysiological stiffness. That is why hydrogels are gaining such interest in the field, they can reach physiological stiffness and they have high water content. However, hydrogels-based microfluidic devices have not been extensively explored so far.

Hydrogels have different physicochemical properties that make them suitable for biomedical applications, such as, they are optically clear for imaging, some of them are inexpensive, they can either promote or inhibit cell adhesion, their mechanical properties are comparable to those of biological tissues, and they can be easily shaped by soft lithography procedures. These, and other characteristics, make them interesting also for microfluidic approaches [12].

Hydrogels have been incorporated in microfluidic applications in different manners. Ling et al. [16] developed open agarose microchannels that were later closed by another hydrogel lid and fused together (Figure 5). Despite its interesting characteristics, the microchannels dimensions only go down to 50 µm in width and 70 µm in height (Figure 6) which is far from the microscale we aim to reach.

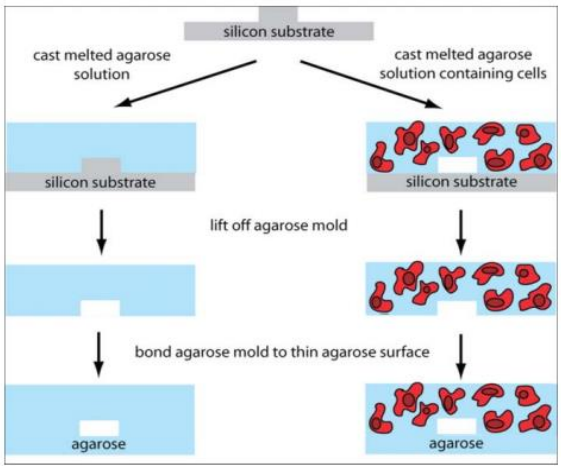

Figure 5: Schematic of the fabrication of agarose microfluidic devices. Adapted from [16]

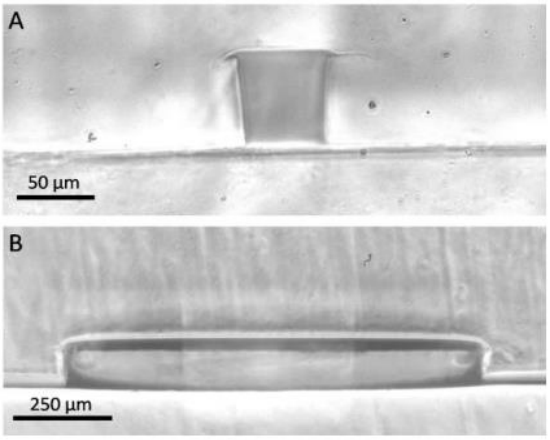

Figure 6: Cross sectional images of agarose channels. A) Channels of 50 um width x 70 um height. B) Channels of 1 mm width x 150 um depth. Adapted from [16].

Choi et al. [17] developed another agarose device which aimed to confine cells with gels of different stiffness. It consisted of a hydrogel lid placed on top of 2D seeded cells. In this case no channels are defined, and cells are seeded on a coverslip, so cells do not sense physiological stiffness in the 3 spatial dimensions but only on top of them.

A different approach is to embed the cells directly inside the hydrogel [18]–[20]. Despite it is a very simple method, it has some throwbacks. It is limited to hydrogels with adhesion motifs, to promote cell attachment and proliferation, and there is also a lack of control over the architectural organization of cells within the hydrogel, as cells may exhibit irregular distribution or random orientation, which can impact tissue development and functionality.

Recently, Afthinos et al. have developed novel polyacrylamide (PA)-based four-walled microchannels of physiological stiffness [21]. It consists of a soft lithography-based compliant microfluidic device with independently tunable stiffness and degree of confinement, and they call it hydrogel-encapsulated microchannel array (HEMICA). They have demonstrated different applications of the device for high-throughput analysis of cell motility. The fabrication methodology they propose is illustrated in Figure 7. Microchannels were fabricated on a silicon wafer which was used as a mold for PA polymerization, the resulting gel had the microchannel design imprinted on the lower surface ("imprinted gel"). At the same time, a flat PA hydrogel was polymerized on an activated coverslip. Once the maximal swelling of gels was acquired (after 2-3 days), the flat gel was coated with bis(sulfosuccinimidyl)suberate (BS3) and the imprinted gel was placed on top and allowed to adhere. Finally, to coat the device with ECM proteins, microchannels were incubated under UV light with Sulfo-SANPAH followed by the addition of the desired protein. This is in line with our goal, and we will get this as a reference for our work.

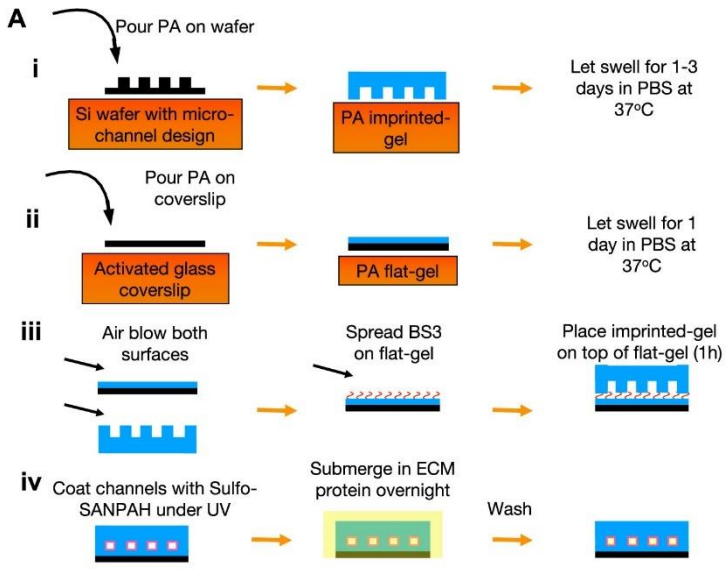

Figure 7: Schematic representation of the production of PA hydrogels with microfluidic tracks, assembly of HEMICA devices, and ECM protein coating. Adapted from [21].

2.2. State of the situation

Microfluidics is the most suitable technique to study the kinetics and migration mechanisms of immune cells. Microfabrication enables to develop constriction microchannels, but in these setups, cells are enclosed in narrow channels, commonly of PDMS, where wall stiffness is much higher than in vivo scenarios. Hence, appear the necessity of fabricating microchannels made of soft hydrogels, which are still an open issue in microfabrication.

We have seen how most of the microfluidic devices that have been developed so far are PDMS-based devices. The options that apply hydrogels in their devices are mostly to study macroscopic level processes.

From this situation, stands a new project in the Biomimetics Systems for Cell Engineering group, which wants to overcome these limitations in hydrogel-based microfluidic devices. "*Hydrogel-based microfluidic toolbox to investigate immune cell recruitment in colorectal cancer (HEROIC)"* project aims to mimic the tumor microenvironment (TME) of colorectal carcinoma, and the migration of immune cells in highly constrained and controlled microenvironments. To do that, two different hydrogel-based microfluidic tools are proposed. The first one will be a microfluidic device that reproduces the intestinal mucosa tissue cross-section with three compartments: epithelial-stromal-endothelial. The second tool must reproduce the constrictions that immune cells must undergo during the path to tumoral region. It must accurately control the mechanical and chemical properties of the narrow structures they pass through.

The current final degree project focuses on the second goal of HEROIC project. As detailed in 1.1. Aim and scope of the project, we want to develop a polyacrylamide (PA) microfluidic device of confined microchannels of tunable stiffness and size. By this way we will be able to mimic the constrictions of the in vivo pathways maintaining stiffness levels similar to physiological ones.

3. MARKET ANALYSIS

The principal interested sectors and stakeholders of the proposed microfluidic device are pre-clinical research field in pharma and biotechnology companies. It can contribute to ADME (absorption, distribution, metabolism, and excretion) and toxicology assays. The *In vitro* pre-clinical tests of drug candidates can save costs, time, and decreases animal testing.

The global market of microfluidics is the most involved in the current project and it was valued at $20.7 billion in 2021 and it is expected to reach $58.8 billion by the end of 2026, with a compound annual growth rate (CAGR) of 23.2% [22].

The microfluidic market can be segmented by product type (microfluidic-based devices, microfluidic chips, pumps, etc.), by application (drug delivery, pharmaceutical, etc.), and by material (polymer, silicone, glass, and other materials) [23]. It can be noticed that hydrogels are not specified as a material option, they would be included in other materials. This proves that they are still not well stablished in the market of microfluidics. The market is dominated by companies like uFluidix, Bio-Rad Laboratories Inc., Fluidigm Corporation, Illumina Inc., and PerkinElmer Inc.

If we look at one of these key players in the industry, for example uFluidix, we see that they are focused on advanced PDMS-microfluidic devices. For example, ready to use microchannels approaches (Figure 8) are available in the market in smaller companies such as 4D Cell Explore Better, they offer a large variety of sizes and constriction designs. They all are powerful in the field but there is not yet an important provider for hydrogel-based microfluidic devices so it could be an interesting business opportunity [24].

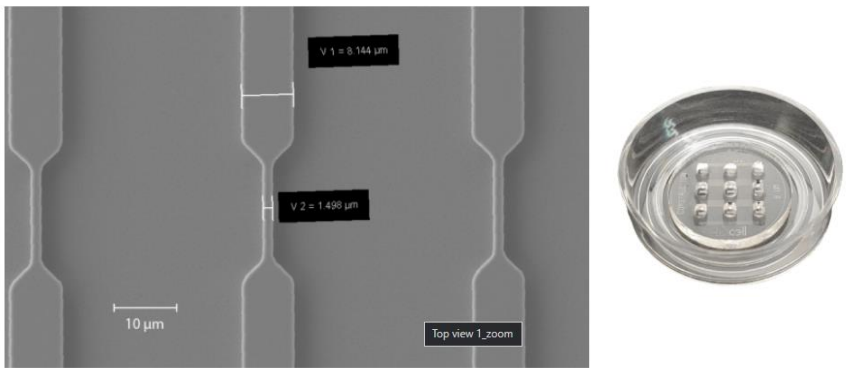

Figure 8: Example of an already to use PDMS chip provided by 4Dcell. Adapted from [24].

It seems that the future of the microfluidics market is highly focused on the emergence of microfluidic-based 3D cell culture systems. There is a huge attention on the ability of replicating tissue-tissue interfaces, and mechanical environments of living organs, and here is where our product can be successful.

Finally, in a secondary plane, the proposed device, could help in the diagnosis of colorectal cancer and thus, reduce the cost of the disease on economic and social aspects.

4. CONCEPT ENGINEERING

In this section we are going to explain in detail all the materials and methods employed during the Project. The different approaches, materials, and strategies that have been considered to acquire the best development protocol and fabricate the desired devices are going to be discussed and the optimization process needed to get it, will also be described in the following parts. Figure 9 shows a general layout of the different steps followed during the project. In the next parts, the different processes involved in each of them will be detailed.

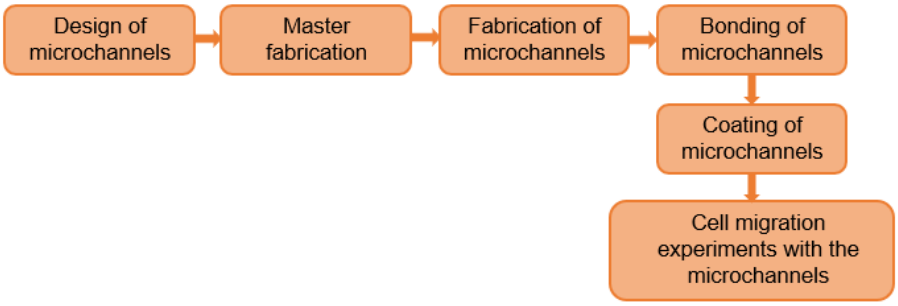

Figure 9: Layout of the different steps of the project.

4.1. Design of microchannels

We wanted to develop a microfluidic device able to perform cell migration experiments. After a bibliographic review, as reported in *2.1. State of the art* section, we decided to design a device formed by two vertical main channels, with four inlets/outlets at the ends (for cell seeding and medium inflow/outflow), and several transversal microchannels connecting the two main ones. Figure 10 shows the scheme of the general design for the device.

4.1.1. Dimensions and geometry

T lymphocytes are small cells of 8 to 10 microns in diameter [25]. They are released to the blood stream, where vessels' diameter can vary from 5 to 70 microns [26], and after that, they have to extravasate through the vascular endothelial barrier and migrate through the tumor stroma till reach cancer cells. Knowing that and considering the resolution of the microfabrication techniques that will be employed, we designed narrow transversal channels that approximate physiological environments.

The dimensions of the whole device were 13 x 5 mm, thought to fit inside a Mattek glass bottom petri dish of 35 mm diameter. On the one hand, straight microchannels of two different lengths (L1 = 200 µm, L2 = 1820 µm), fixed height (H = 5 µm), and widths of 5, 10 and 15 µm were designed as transversal channels to connect the two main channels. On the other hand, to have more variability of devices and to allow different cases of studies, transversal microchannels of different shapes and constrictions were also considered. This time, transversal channels were of fixed length and height (L2 = 1.82 mm, H = 5 µm), widths varied between 5 and 15 µm and constrictions up to 4 µm were created. Regarding the main channels for cell seeding and media inflow/outflow, they were common for all the previous designs, with a height of 50 µm and a width of 500 µm. Inlets and

outlets were circular features of 1.5 mm diameter. Figure 10 displays the different microchannels designs.

4.1.2. Design Software

The design of microchannels started with the design of the photomask for the later photolithography process. Among the different design software available, the following ones were took into account.

- AutoCAD: AutoCAD is computer-aided design (CAD) software that is used for precise 2D and 3D drafting, design, and modeling with solids, surfaces, mesh objects, documentation features, and more. It is commonly used for photomask design among many other applications. But since it is not exclusively focused on mask design it could be hard to learn it [27].
- CleWin: CleWin is a hierarchical layout editor, it has evolved from a simple editor to a powerful mask design tool. It is compatible with other layout software since it uses the standard CIF, GDS-II, and OASIS file formats. Furthermore, CleWin can read and write the AutoCAD DXF format. High resolution (Encapsulated) PostScript is available as output format. Because CleWin is also meant to be used by students it provides a user-friendly interface [28].
- Freehand: Adobe FreeHand is a computer-based application that allows creating two-dimensional images for illustration and web content. The application is similar to Adobe Illustrator, Corel Draw and other designing apps. The software helps in the creation of illustrations for creative design and layout of print with an unmatched set of creative design tools [29].

Finally, CleWin was used for the photomask design. It has many advantages since it is developed for mask designing and it is the most user-friendly among the three described above. Other members of the group already had experience with this software, and this also made us opt for it. The previously described designs were implemented with CleWin. Since the microfluidic design will have two layers (main channels of 50 µm in height and transversal channels of 5 µm in height) these will be implemented as two different layers in Clewin. The first layer corresponds to the horizontal main channels, and the second layer contains the transversal microchannels. Furthermore, to be able to align the masks for the two layers, the alignment motifs, provided by the Micro Fabrication unit of IBEC, were added to the design, the two-layered fabrication methodology will be explained in depth in the following section 4.2.1. Microfabrication techniques.

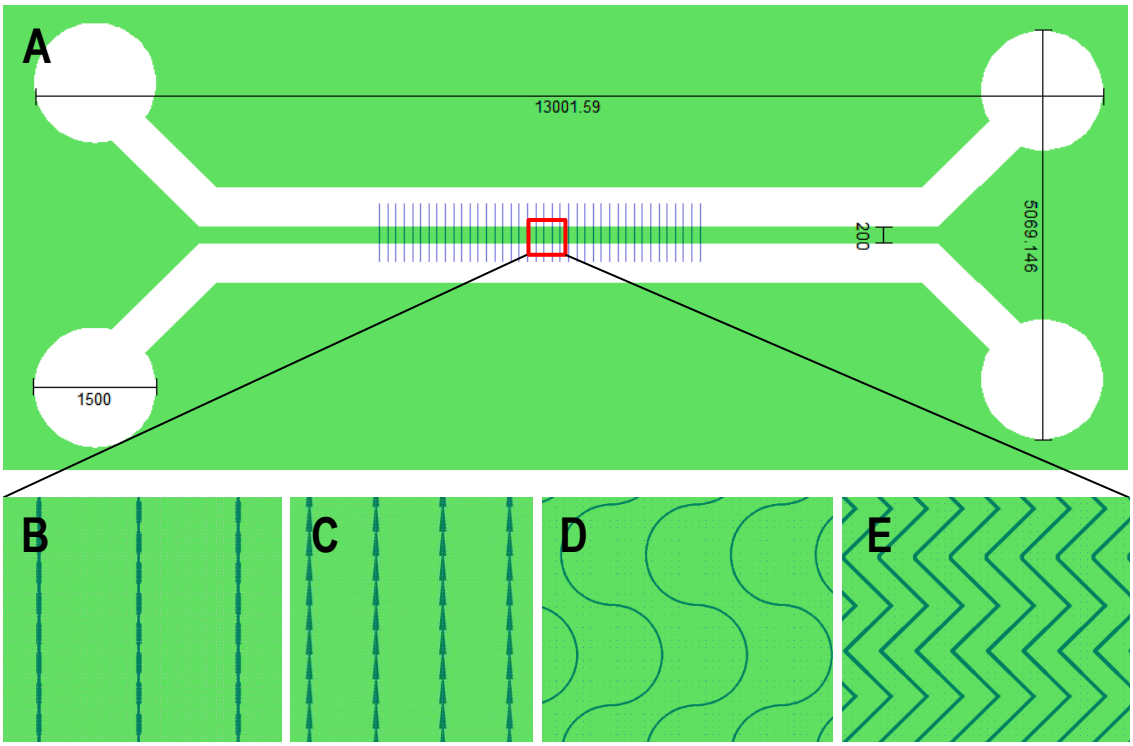

Figure 10: CleWin designs of the microchannels. A) Scheme of the whole microfluidic device with dimensions expressed in micrometers. B, C, D, E) Zoom in of the different microchannels designs. With constrictions, ratchet, wavy and zigzag microchannels, respectively.

4.1.3. Photomask fabrication

Once the designs are corrected and verified, masks have to be ordered to a mask making company, to follow with the lithography process. The first layer contains smaller features up to 4 µm, for that reason its fabrication requires from a high-resolution technique, which will be completely driven by Micro Fabrication unit of IBEC. Regarding the second layer, its smallest feature is of 40 µm, so it can be done by a conventional photolithography technique. Therefore, the second layer of both designs was sent to JD Pohotodata, a mask making company, to acquire the corresponding photomask and use them in a later mask lithography process.

4.2. Fabrication of microchannels

With the final designs established, we were able to start manufacturing the microfluidic device. The fabrication process includes different steps. The process starts with the fabrication of the SU-8 master with the microchannels designs, through a lithography technique. From this master, we can obtain either PDMS or PA replicas of the patterns and get the microchannels imprinted in the desired material. Since the goal is focused on obtaining confined microchannels, at the same time, flat gels or glass slides are also prepared to have a surface where we could bound the microchannels. Finally, the last step aims to create four walled structures, by bonding the microchannels to the flat surface, obtaining, thus, the arrangement of the final microfluidic device.

4.2.1. Microfabrication techniques

The ability to manufacture a wide variety of materials into even smaller device is thanks to the progress in micromachining and other fabrication techniques. The list of fabrication methods for different types of materials and applications has become so extensive. Next, we are going to list

different microfabrication techniques used in microfluidics and similar applications, and we will explain the selected ones in our fabrication process.

- Micro-mechanical cutting: has emerged from the arrival of high-precision machining. It is suitable for the fabrication of individual personalized components instead of a large group of pieces, which will result too expensive. Nevertheless, it provides good surface finish and form accuracy, the process can be done at high speed, it can be used for a large number of materials, such as steel, aluminum, plastics, and polymers, and does not require a very expensive setup. An important disadvantage of mechanical cutting is the damage produced by the cutting tool what can generate cracks [30].
- Photolithography: The most widely used form of lithography is photolithography, which is based on pattern transfer from a mask onto thin films. It has been extensively used in the fabrication of semiconductors to construct Integrated Circuits, and Micro Electromechanical Systems (MEMS). Microfluidic chips are fabricated by photolithography in a similar way to that of semiconductor chips. These silicon-based chips are robust and have been used for several biomedical applications. Disadvantages of the technique are related to the inability to pattern non-planar three-dimensional structures, that is why scientists turn to soft lithography in these cases [31].
- Laser lithography: It consists of a high-precision, highly flexible technology used in environments where rapid prototyping of features sized greater than 1 μm are required. This maskless photolithography enables the transfer of the design directly to the wafer without the need for a photomask. The pattern is exposed onto the substrate with the help of a spatial light modulator, which acts as a “dynamic photomask” [32].
- UV-laser microchanneling: Photons of UV lasers have very high energy; the material ablation takes place by means of electronic excitations which causes the ionization by breaking chemical bonds between the atoms. This kind of material removal phenomenon is called photoablation. UV lasers require specially designed optics, beam delivery and diagnosis. Excimer lasers often require mask to produce microchannels to selectively etch the surface. Most of the UV lasers and excimer lasers have been specially used for polymeric material [30].

As we have already commented we designed a two layered microchannel device. Two-layered photolithography may often be interesting to have different sizes of structures on the same mold, as, for example, series of small channels bridging larger ones in which fluids can be flown without imposing any flow on cells inside small channels, and thus, two masks are needed for each one of the layers [33]. Therefore, the two layers would require different grades of precision in the fabrication process, so, different microfabrication techniques were employed for the fabrication of each one of them. The first layer was fabricated by a Direct Write Laser (DWL) Lithography, because, as reported before, it is able to perform features of sizes up to 1 μm, and this layer had the microchannels designs, where the minimum feature was of 4 μm, so better resolution would be obtained with laser lithography. For the case of the second layer, the minimum feature was of 40 μm, no high-resolution technique was required in this case, so photolithography was the fabrication method used. The photomask was ordered at JD Photodata and the photolithography process was developed by a UV Photolithography Mask-Aligner. The Si wafer obtained from the first process of

DWL, for the first layer, was the starting point for this second fabrication process. The whole master fabrication process was done by Micro Fabrication unit of IBEC.

4.2.2. Materials

Regarding the material which the microchannels are made of, we must take into account the objectives and requirements we set at the beginning of the project for our device. We wanted a microfluidic chip that mimics the tumor microenvironment and replicate, to the greatest extent feasible, the mechanical characteristics of the cellular surroundings. To accomplish that, the following materials have been considered.

4.2.2.1. PDMS

PDMS is one of the most common materials used for fabrication of microfluidic devices. They are extremely versatile and have been applied for the culture of different cell types. However, they can be limited by the properties of PDMS as a material. Sealing of the system, to acquire confined microchannels, for example, is performed by plasma treatment which can alter other complementary treatments needed for cell compatibility. Furthermore, PDMS is not permeable to aqueous solutions, and this can lead to local medium heterogeneities and accumulation of cells or residues. Finally, and decisive for the goal of this project, PDMS has poorly tunable mechanical properties, and have supraphysiological stiffness. Many of these issues can be addressed using hydrogels, that is why we have considered polyacrylamide as a potential candidate for the project [34].

4.2.2.2. Polyacrylamide

Hydrogels, particularly polyacrylamide gels, offer numerous advantages for developing devices in biological studies. They promote uniform diffusion of the medium, ensuring a consistent cellular environment. These gels require minimal technological investment, they are well-characterized and known to be biocompatible. Compared to other gels, like agarose, polyacrylamide gels exhibit greater mechanical strength, enabling, thus, easier handling what makes them suitable for microfabrication. Additionally, their mechanical properties can be easily tuned across a wide range. By adjusting the ratio of acrylamide to bis-acrylamide components, the stiffness of polyacrylamide hydrogels can be simply modified. Furthermore, these gels can be functionalized with proteins to mimic the composition of the native extracellular matrix (ECM) and enhance their bioactivity [34].

Table 1: PDMS and PA comparison for microfluidic applications. Green means advantage and red throwback. (-) means lack of characteristic. (+) means grade of presence of the ability / defect.

	PDMS	PA
Transparency	+++	+++
Flexibility and elasticity	+++	+
Water permeability	-	+++
Biocompatibility	+++	+++
Well-stablished fabrication techniques	+++	-
Fabrication complexity	+	++
Tunable mechanical properties	+	+++
Biomimetic properties	+	+++
Bonding protocols	+++	-
Swelling and stability	-	+++
Deformation and damage	-	++

In Table 1 we can see a sum up of the different properties, advantages, and disadvantages that both materials show. Polyacrylamide (PA) hydrogel was the one that better suits for the project proposals. As previously mentioned, PA hydrogels' stiffness can be easily modified and closer physiological stiffnesses can be achieved comparing with PDMS. Even though PA was chosen for the fabrication of the microchannels, we parallelly worked with PDMS. PDMS protocols are better stablished, and its manufacturing and handling is easier and better known as the case of PA. For that reason, we decided to develop at the same time both PA and PDMS microchannel devices in order to benchmark the new approach of PA microchannels fabrication, and to optimize the cell migration experiments set up.

4.2.3. Microchannels obtention

With the fabricated master obtained by the Micro Fabrication unit of IBEC, we already had the template for the microchannels which were obtained by different ways for the case of PDMS and PA. Soft lithography and capillary force lithography procedures were used respectively. Next, we explain the different procedures implemented to develop the microchannels, the issues that each one presented and the final selected protocols.

4.2.3.1. PDMS microchannels

To get the PDMS microchannels we employed a simple process of replica molding (Figure 11). We made a PDMS replica of the negative master with the microchannels designs. We first prepared the PDMS solution with PDMS precursor and curing agent at a ratio of 10:1 and mixed it with a Pasteur pipette for 5 minutes. After that, we left the solution degassing for 30 minutes, to eliminate all the bubbles. The solution was then poured on the master's covering all the surface. If there are still some bubbles, it can be left under vacuum again for 30 minutes more or try to remove them blowing with the help of a Pasteur pipette. The PDMS was then cured overnight (o/n) at 80 - 85 ºC.

Finally, to get the microchannels, we demolded the PDMS from the master with the help of a scalper and tweezers and cut every single device. Furthermore, with a puncher of 0.75 mm diameter we

opened the inlets and outlets. The device was then ready to be bonded to a flat surface to form confined microchannels.

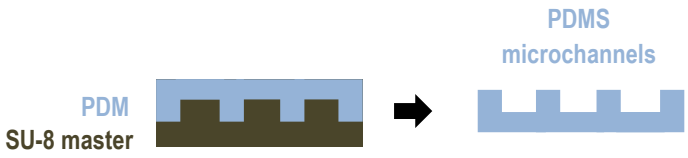

Figure 11: Scheme of the fabrication of PDMS microchannels, from the master designs.

4.2.3.2. PA microchannels

For the case of PA microchannels two different fabrication methodologies were developed and optimized. Both are based on the concept of Capillary Force Lithography (CFL). CFL is a nanofabrication technique that involves the self-assembly of liquid materials to create patterns on a solid substrate. The process begins by depositing a thin layer of a liquid onto the substrate, followed by placing a template with desired pattern on top. The capillary forces between the liquid and the template cause the material to flow and fill the gaps in the template, resulting in the replication of the pattern on the substrate. After the material solidifies, the template is removed, leaving behind the desired pattern [35]. The purpose in here was to create micro structured PA hydrogels using CFL. This is usually done by using silicon hard molds, but this makes difficult the demolding of the hydrogel and can damage the imprinted structures. Knowing that we designed an alternative process based on the fabrication of flexible PDMS molds which allowed for an easier detachment of the structured hydrogel [36]. Furthermore, the PDMS acts as a source of oxygen, which inhibits PA polymerization, that is why we need to employ very thin layers of PDMS to be used for PA molding. The process, then, involves several PDMS replicas to get the final mold. Even so, the common method was also employed, the direct fabrication of PA from the SU-8 master was the second attempt for the obtention of imprinted PA hydrogels. Both processes are detailed below.

4.2.3.2.1. PDMS replicas fabrication method

As explained before, this process consisted of the creation of flexible PDMS thin molds to be used for the patterning of PA hydrogels, an scheme of the different steps followed is seen in Figure 12 and Figure 13. The first step was to obtain a PDMS replica from the master, following the same procedure as in *4.2.3.1. PDMS microchannels*. These PDMS replica (PDMS1) had the same shape as the final PA hydrogel, so we needed a negative PDMS mold (PDMS2) to obtain the final PA hydrogel. The PDMS1 replica was demolded, and every single device was cut and separated. Then, each device was bonded on a glass slide by plasma activating both, the surface of the glass and the surface of the PDMS1 device without the patterns, therefore the channels were looking up and could be used as a mold. Once these molds were bonded, the top surface was silanized. The silanization is necessary because we want to obtain a contra replica of PDMS from these molds, the silanization allows that the PDMS2 replica can be peeled off from the PDMS1 mold easily. This silanization process consisted in another plasma activation of the surface which needed to be silanized. Then, during the first 15-20 minutes in which the activation is maintained, we placed the PDMS1 molds and two coverslips in the desiccator. Around 150 µl of Trichloro(1H,1H,2H,2H-

perfluorooctyl) silane (PFOCTS) were dropped on the glass coverslips and left on vacuum for 2 hours, this created an atmosphere with the silane in vapor phase. The silane molecules are then deposited on the activated surface of the PDMS1 mold. After that, the molds were left on the oven at 65ºC for 2 hours more to order the self-assembled silane monolayer. The second step was to make a contra replica of PDMS from the current molds. But this time the replica needed to be very thin in order to minimize to the most the source of oxygen form the PDMS. To achieve that, we used a spin coater. A thin layer of PDMS was spin coated on the previously developed PDMS1 molds. To acquire the desired thickness the setting parameters of Table 2 were used. After the coating the molds were left in the oven over night at 85ºC. Finally, the thin layer of PDMS was demolded and placed on a squared glass coverslip with the design looking up, and the final flexible PDMS2 mold was ready to be used for PA patterning.

Table 2: Spin coater program settings.

Steps	Time (seconds)	Velocity (rpm)
1	5	500
2	60	1000

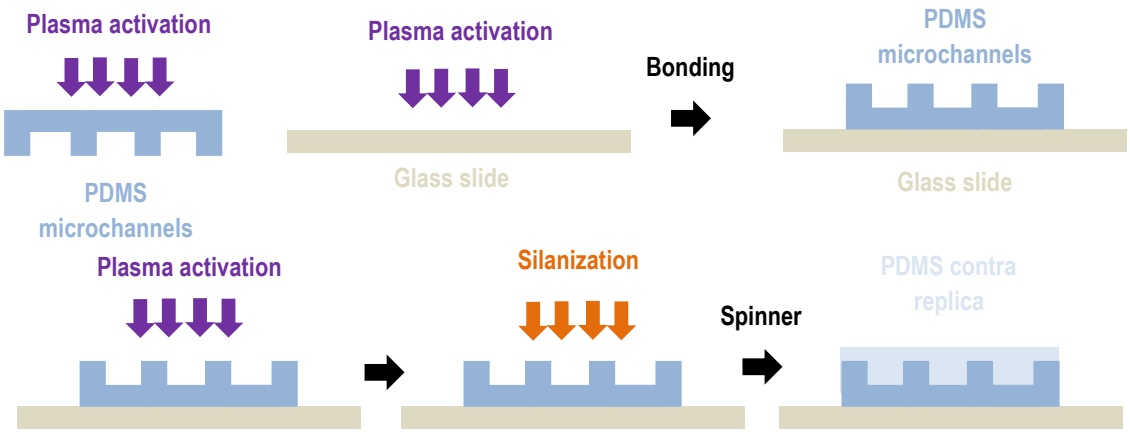

Figure 12: Scheme of the PDMS thin mold acquisition.

In that point, we were able to fabricate the micropatterned PA hydrogels using the obtained molds. To do that, PA solutions need to be previously prepared. We worked along the project with three different PA hydrogel stiffnesses, 8 kPa, 15 kPa and 21 kPa. The three different solutions were prepared mixing different concentrations, as reported in Table 3, of acrylamide (Bio-Rad, 40%) and N,N-Methylene bisacrylamide (Bio-Rad, 2%), as previously defined [21]. The mixtures were degassed for 10-20 minutes and then, 10% ammonium persulfate (APS) dissolved in MiliQ, and N,N,N',N'-tetramethylethylenediamine (TEMED) were used as initiators of polymerization. For 297µl of PA solution, 3µl of APS and 0.9µl of TEMED were added. The remaining PA solutions were kept in fridge until be used again. To obtain the imprinted PA hydrogels, 1 ml of the prepolymer solution was poured into squared PDMS pools of 3 mm height placed on a glass coverslip. Then, the coverslip with the PDMS thin mold was rapidly placed on top of the solution. Hydrogels were left at room temperature (RT) for 2 hours to polymerize. After these 2 hours, the top coverslip with the mold was peeled off carefully and the PA hydrogel was submerged in PBS and kept in fridge for 2-3 days to let it get the equilibrium swelling.

Table 3: Polyacrylamide hydrogels composition for each stiffness.

PA stiffness (kPa)	Acrylamide %	Bisacrylamide %
8	8	0.1
15	8	0.2
21	8	0.6

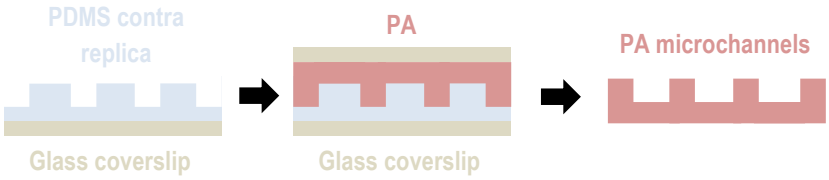

Figure 13: PA polymerization on PDMS thin molds scheme.

4.2.3.2.2. SU-8 master fabrication method

The other method employed to obtain the imprinted PA hydrogels did not have as many steps as the previous one. It consisted of obtaining a PA replica directly from the designs in the SU-8 master (Figure 15). To do that, we firstly covered the master with PDMS and let it cure o/n at 80-85ºC. Instead of demolding the PDMS replica of the master, this time we only demolded the PDMS from the single devices we wanted to obtain a PA replica. Leaving, thus, a pool with PDMS spacers with the designs on the bottom surface (SU-8 master), as it can be appreciated in Figure 14. Secondly, 1 ml of the PA prepolymer solution, prepared in the same way as explained in the previous section, was added in the pool and a glass coverslip was placed on top to add some pressure and facilitate the patterning of the PA hydrogel by CFL. Hydrogels were left 2 hours at RT to polymerize and then were demolded and kept with PBS in fridge, to get maximum swelling, for 2-3 days.

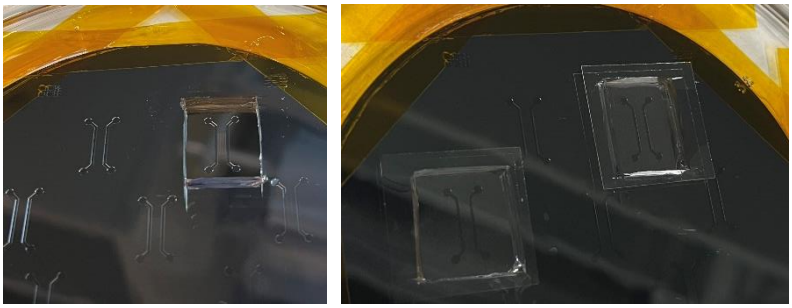

Figure 14: PA imprinted hydrogels fabrication using the SU-8 master as a mold with the microchannels designs for the polymerization.

Figure 15: Scheme of PA microchannels obtention from a direct molding of the master.

4.2.3.2.3. Flat PA hydrogels fabrication method

Concurrently to the fabrication of PA imprinted hydrogels, those with the microchannels designs imprinted on them, we were also fabricating flat PA hydrogels. As the final goal was to obtain 4-walled confined microchannels of PA (Figure 18), we needed a flat PA hydrogel to close the 3-walled microchannels imprinted on the PA hydrogels already fabricated. For the fabrication of flat hydrogels, we always used the same simple methodology, depicted in Figure 16. We started silanizing a squared glass coverslip, with a protocol that employed glutaric dialdehyde 25 wt. % in H2O (glutaraldehyde solution) and (3-aminopropyl) trimethoxysilane 97 % (silane) to form a self-assembling monolayer (SAM) of silane molecules that promotes adhesion to the surface. First of all, 200µl of Silane: MiliQ at 1:1 proportion were added to the coverslip surface and incubated for 5 minutes. After that, 2 ml of MiliQ were added, and it was incubated 30 minutes shaking at RT. It was then rinsed with MiliQ, and 2 ml of Glutaraldehyde solution: MiliQ at 1:50 concentration were added and incubated again for 30 minutes more. Finally, it was rinsed with MiliQ and dried with nitrogen. After silanization, 100 µl of PA prepolymer solution were dropped on the coverslip and it was sandwiched by another non-activated coverslip. We let it polymerize for 2 hours at RT and then we demolded the top coverslip and we had the flat PA hydrogel attached to the glass coverslip surface. We submerged it in PBS and kept in the fridge to let it swell for 2-3 days.

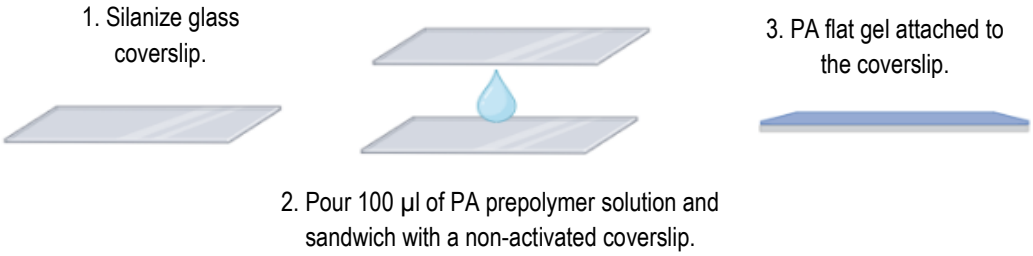

Figure 16: Flat PA hydrogel fabrication process.

4.2.4. Arrangement of confined microchannels

The arrangement of confined microchannels wants to achieve a final, practical microfluidic device, able to perform cell experiments. As explained in the introductory section, one of the goals of the project was to get confined microchannels because it approaches the in vivo conditions at which cells are exposed inside human body vessels. At this point we had both PDMS and PA 3 walled microchannels and we wanted in this part of the work to close these channels by bonding and sealing the current devices to a flat surface. Different procedures were followed for the case of PDMS and PA, and we are going to explain them below.

4.2.4.1. Bonding of PDMS on glass

Silicon-based materials (e.g., glass or silicon) can be relatively easily bonded to PDMS via simple surface activation (Figure 17), and thus these are the most widespread ways of closing the microchannels to form a chip. Both surfaces are oxidized by plasma before contact (in a plasma cleaner for 1 min), the plasma oxidizes the surface to silanol (Si-OH) and then both surfaces are put in contact forming covalent O-Si-O bonds. The plasma-oxidized surface remains hydrophilic if

it stays in contact with water, but in air, rearrangements occur within 30 min, so both surfaces must be placed in contact within this period [37], [38].

We performed the PDMS - glass bonding by surface activation in a clean room. With the PDMS devices already demolded, cut and with the inlets/outlets done, we cleaned them in the chemical bath, first with soap and water and then with ethanol in a sonicator. We left them on a hotplate at 80ºC to ensure the bonding surface was clean. After that we activated the bonding surface of the PDMS and the bottom surface of a Mat Teck glass in a Plasma Cleaner for a minute and we rapidly brought them in contact to form a covalent bonding. To make the chemical link easier after the contact between the PDMS and the glass, it is recommended to heat the set [39]. We left the chips at 65 ºC o/n.

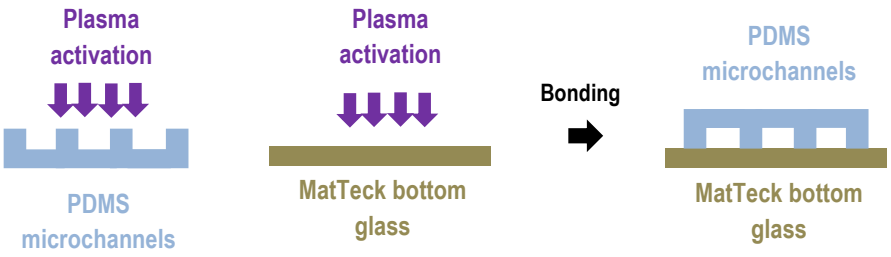

Figure 17: Bonding of PDMS on Mat Teck bottom glass by plasma activation.

4.2.4.2. Bonding of PA hydrogels

In this section, the goal was to obtain confined PA microchannels. With that, cells could have a 4-walled environment of physiological stiffness, different from what they sense in the case of PDMS chips. Devices of homogeneous or heterogeneous stiffnesses could be acquired by using imprinted and flat hydrogels of different stiffness. However, the technologies and protocols for the bonding of two PA hydrogels are not as well stablished as the ones for PDMS. Some approaches have been reported in literature, as seen in *2.1. State of the art* section, but still is a poor explored technique and we have been dealing with several issues with it. Next, we detail three different attempts that have been tried.

4.2.4.2.1. BS3

A novel device, with the desired characteristics specified above, has been previously developed [21]. They reach a bonding between two PA hydrogels using bis(sulfosuccinimidyl)suberate (BS3) as an adhesive. See *2.1. State of the art* section. BS3 is the water-soluble analog of DSS (disuccinimidyl suberate), an homobifunctional N-hydroxysuccinimide ester (NHS ester). NHS esters react efficiently with primary amino groups (-NH2) in pH 7 to 9 buffers to form stable amide bonds. The reagent is commonly used for crosslinking proteins or for intra- and extracellular crosslinking [40].

The reported protocol consisted of preparing the BS3 solution at a concentration of 50 mg/ml and spreading 15 µl of solution on the flat PA hydrogel. Then the imprinted gel was placed atop the flat gel and allowed to bond for 1 hour at RT (Figure 18). Before the bonding, the excess PBS was removed from hydrogels with compressed air. Since we did not obtain successful results from these indications, see the results section in 5. DETAILED ENGINEERING, we started an optimization

process by adjusting different steps and processes of the protocol, they are summarized in Table 4 and explained below, and some of the approaches tried are depicted in Figure 20.

1. Adjust the pH of the reaction: We saw in BS3 datasheet that the reaction is efficient in pH 7 to 9 [16]. In this case, the BS3 solution was prepared with an HEPES buffer solution (pH 7-9), at 50 mg/ml concentration + 20mM HEPES. The rest of the protocol was the same.
2. Amount and spreading of BS3 solution: The bonding was also tested using different amounts of 'adhesive' solution. The indicated one, from the protocol we were following, was 15 µl. Since we did not get successful results, we tried the bonding with 24 µl, 50 µl, and 75 µl. Furthermore, instead of only adding the drop of solution and bringing both gels in contact, we spread the solution with the help of a sheet of parafilm to ensure that all the surface was coated.
3. Time of bonding: The bonding was supposed to be made in 20 min at RT. We also experimented different bonding times, always at RT. We left different gels bonding for 20 minutes, 1 hour and some were left o/n at RT.
4. Quality of hydrogels: The quality of the fabricated hydrogels has a decisive role in the success of the bonding. To get the bonding, hydrogels need to be completely flat and dried. Gels must not have any bubble and during the bonding the contact between both surfaces needs to be perfect and flat, without bubbles in the middle. To achieve that, different fabrication methods for the PA hydrogels, explained in previous sections, were tested.
5. Pressure during bonding: In one of the attempts, we compared the effect of adding some pressure during the bonding, by placing a coverslip and an empty vial on top of the gels.
6. Filling approach: When hydrogels seemed to be bonded, we added ink inside the channels, through the performed inlets, to test it. Usually, hydrogels detached when we were injecting ink, so we thought in alternative ways of injecting it, to exert less pressure and maintain the hydrogels bonded. At the beginning, we were adding ink directly with the tip of a pipette. We tried then to insert cannulas with tubes inside the inlets and connect them to a syringe which in turn was connected to a syringe pump. With that we injected ink at different flow rates 10 µl/min and 5 µl/min.

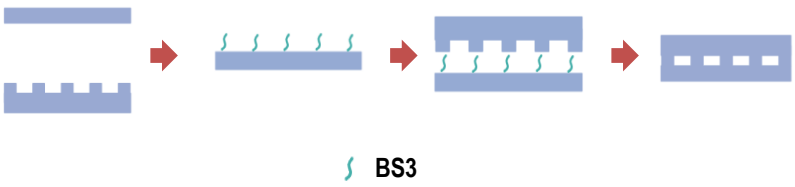

Figure 18: Bonding approach with BS3 as adhesive.

Table 4: Set of parameters studied during the optimization process of bonding with BS3 and Sulfo-SANPAH (SS).

Parameter	Options			
pH	Without HEPES		With HEPES	
Amount of adhesive solution	15 µl	24 µl	50 µl	75 µl
Time of bonding	20 min	1 h	o/n	
Quality of gels	Replicas fabrication method		Direct fabrication methods	
Pressure during bonding	Without pressure		With pressure	
Filling approach	Pipette	Syringe	Syringe pump	
Concentration of adhesive solution	Same molar concentration as SS		50 mg/ml	

4.2.4.2.2. Sulfo-SANPAH and diamine

After all the optimization process commented above, still we did not obtain a good and permanent bonding of the PA hydrogels, so we developed a new methodology based on Sulfo-SANPAH activation of gels' surfaces and bonding with a diamine. This new attempt aimed to improve the chemical part of the procedure. Sulfo-SANPAH is a heterobifunctional crosslinker that contain an amine-reactive (NHS) ester and a photoactivatable nitrophenyl azide [41]. It is commonly used to conjugate proteins in the surface. Sulfo-SANPAH is adhered to the PA surface by its photoactivatable side, and the other extreme which remains free is an NHS ester, which reacts with primary amino groups. So, the idea was to bind, the two gels, which would have these free NHS esters extreme, after Sulfo-SANPAH activation, with a diamine molecule, which in turn has an amino group in both extremes and could, thus, react with Sulfo-SANPAH and maintain both gels bonded. The diamine molecule chosen was 1,6-Diaminohexane, which had the same chain length as BS3. Our approach is illustrated in Figure 19, which consisted of activating the surface of both, the flat and the imprinted gel by adding 200 µl of Sulfo-SANPAH solution and leaving it to react under UV light for 5 minutes. Then we washed the remaining solution with PBS and dried the gels with compressed air. At the same time we prepared the diamine solution, which would serve as an adhesive, with the same concentration as BS3 (50 mg/ml), and then we added 50 µl of solution to the flat gel and we brought the imprinted gel on top and let it bond. The same optimization process as before, was employed in this case. The different parameters recapped in Table 4,such as time of boning, filling approach, amount of solution, presence of pressure during bonding and quality of hydrogels were considered also for this approach, and furthermore, the concentration of the "adhesive" solution was also tunned. We first tried to prepare a diamine solution with the same molar concentration as the Sulfo-SANPAH, and then we turn to the same concentration used for the BS3.

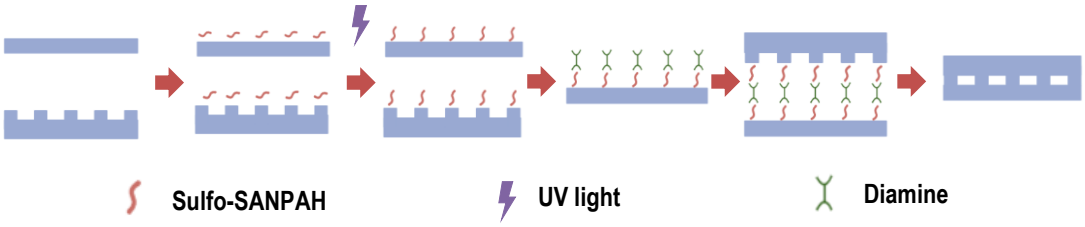

Figure 19:New hydrogels bonding approach with Sulfo-SANPAH + diamine.

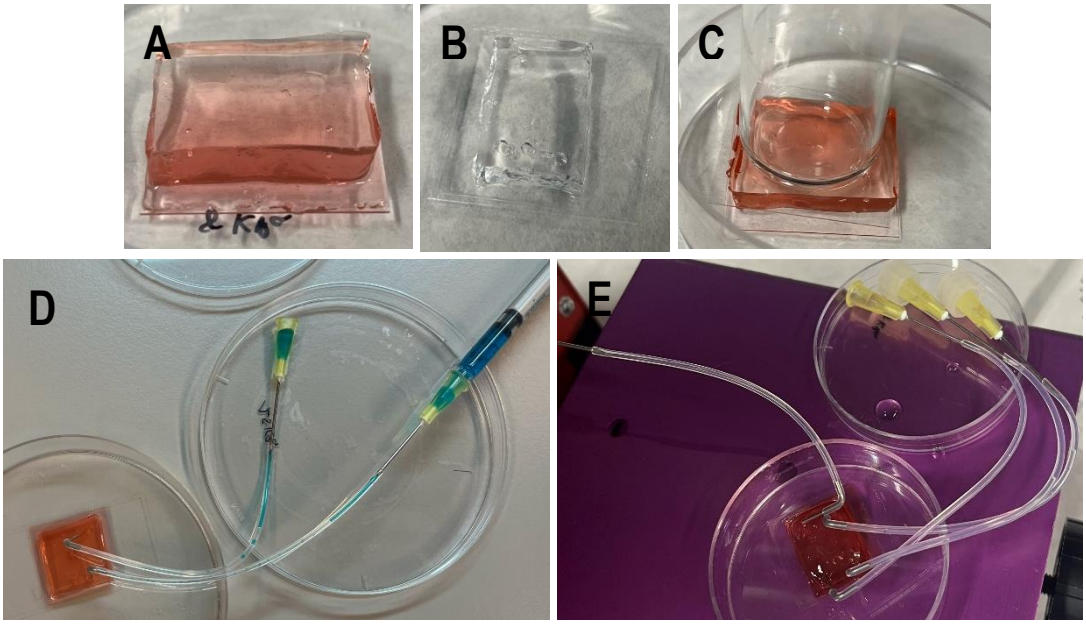

Figure 20: Different PA hydrogels bonding trials. A) Bonding with Sulfo-SANPAH and diamine. B) Bonding with BS3. C) Bonding with pressure. D) Filling the channels with syringe. E) Filling the channels with syringe pump.

4.2.4.2.3. Mechanical arrangement

The last attempt was to arrange the device mechanically, by bonding both gels by force instead of using a chemical approach. The idea was to enclose the device (PA flat gel + PA imprinted gel) between two polymethyl methacrylate (PMMA) layers, separated by a PDMS spacer of the same thickness as the imprinted hydrogel. Then, make a mechanical clamping between the two layers, making pressure on the PDMS frame, not on the gel. Figure 21 shows the scheme of the designed casing for the hydrogels.

We first cut two PMMA layers, we placed the coverslip, with the flat PA hydrogel attached on it, on one of the PMMA layers. We add on top of the coverslip a PDMS frame (pool) and inside it we placed the PA imprinted gel, with the microchannels looking down. The PDMS frame had the same dimensions and thickness, approximately, then the PA imprinted gel, in order to assure the hydrogel does not move. Then, we made holes in the remaining PMMA layer, to make them fit with the inlets/outlets of the hydrogel. Finally, we placed the PMMA layer on top and clamped all the device with two clips, by the PDMS spacer parts.

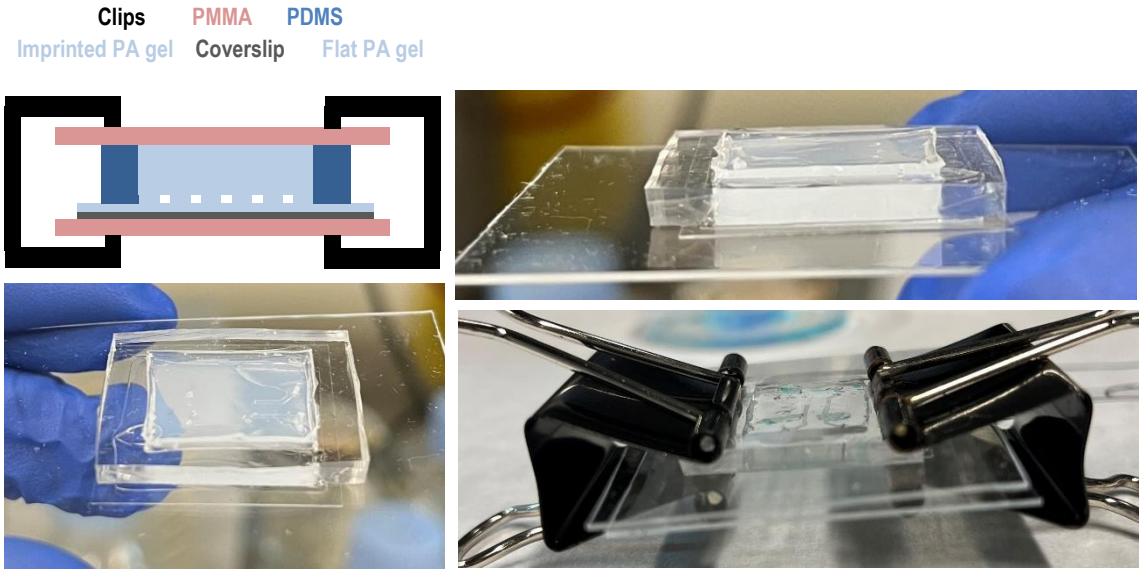

Figure 21: Scheme and implementation of the mechanical arrangement.

4.2.5. Cellular component

We are going to discuss now the cellular component of the project. Once the microfluidic devices are finished, experiments with cells can be performed. Cell experiments and cell migration analysis were not part of the principal goal of the work. The aim of the experiments was to test the performance of the developed microfluidic devices. We explain below the experiments that have been realized and the different designed setups.

4.2.5.1. Cell type

Two different cell lines were employed for the different experiments.

- *NIH 3T3*

These cells are a mouse embryonic fibroblast cell line, which are a type of connective tissue cells that are involved in producing the extracellular matrix and providing structural support to tissues. These adherent cells have the ability to divide rapidly and can be easily cultured in the laboratory [42]. The medium used for culturing NIH3T3 cells has been Dulbecco's Modified Eagle's Medium (DMEM Medium) (Gibco) supplemented with 10% (v/v) of Fetal Bovine Serum (FBS) (Gibco) and 1% of (v/v) Penicillin/Streptomycin (Pen/Strep) (Sigma-Aldrich). Flasks have been incubated at 37°C in 5% CO2. Cells were split when reached approximately 80% of confluency, every 2-3 days. The steps followed to split cells were, first of all, aspire the media, then, clean with 5 ml of PBS and aspire it. Detach cells with 1 ml of trypsin and leave 5 minutes in the incubator. Add 4 ml of cell media and pass all the culture to a 15 ml flask to centrifugate 5 minutes at 1200 rpm. After centrifugation, the media is removed, and the supernatant is resuspended in 5 ml of fresh media. Finally, a new culture flask is prepared with 1/5 proportion of cell solution and cell media, respectively.

- *Jurkat*

Jurkat cells belong to a type of human T lymphocyte (T cell) line and are often used as a model system to study different aspects of T cell biology and immune responses. They are particularly used in this laboratory for T cell migration studies [43]. They grow in suspension and do not adhere to surfaces, unlike NIH 3T3 cell line. Jurkat cells were cultured and expanded in Gibco RPMI Medium 1640 (1X) + GlutaMAX-I supplemented with 10% dialyzed fetal bovine serum and, 1% (v/v) Pen/Strep. They were incubated at 37°C in 5% CO2. These cells were cultured in collaboration with other members of the group and their own protocols were followed for the split of the cells.

4.2.5.2. Cell seeding on PA hydrogel

First, we wanted to see how cells were behaving on PA hydrogels in comparison to when they sense a stiffer surface such as glass. To do that, we prepared an experiment which consisted in developing two PA flat hydrogels of 21 kPa stiffness on squared coverslips. The top surface of gels was functionalized. First, the surface was coated with 200 µl of Sulfo-SANPAH at a concentration of 2 µg/µl in Milli-Q water and activated with UV light for 1 minute, till we saw a change in color from red to brown. We rinsed the surface with PBS and then we added 100 µl of 1 mg/ml fibronectin solution. We left it 1 hour to act and then we rinsed again the surface with PBS. We placed both gels in a 6-well plate (Figure 22). We prepared a 1/20 3T3-GFP cell solution, and we added 2 ml of solution to each well. We seeded cells on gels and, also, on an empty well, without hydrogel, as a control. We left it in the incubator and then we performed a time-lapse video o/n.

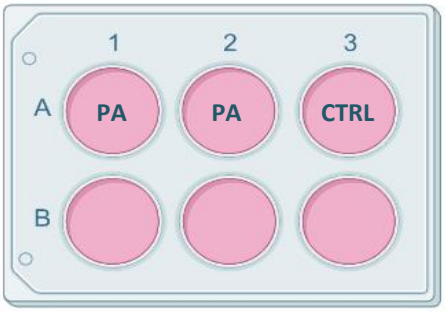

Figure 22: 3T3 cell seeding on PA hydrogels experiment design.

4.2.5.3. 3T3 on PDMS microchannels

This was a first attempt on using the designed microchannels, in this case the PDMS ones. The PDMS chips were fabricated as explained in section 4.2.4.1. Bonding of PDMS on glass. We used 15 µm width, short channels. We filled the channels with 20 µl of cell media, inserting the tip of the pipette in the performed inlets, and then we added 20 µl of cell solution (1/5), from our culture of NIH-3T3, using the pipette. We finally covered the chip with 3 ml of cell media, and we left the chip in the incubator o/n.

4.2.5.4. Jurkat on PDMS microchannels

Jurkat cells were the dedicated cell type to study the migration of T-cells. Several experiments were done with Jurkat cells using the PDMS microchannels. Short 5 µm width microchannels were employed for these set of experiments. The preparation of cells was always the same. Cells were counted, and a sample of 5 million cells was taken. Cells were dyed with PKH26, which is a membrane dye compatible with live-cell culture, and they were kept in incubator till cell seeding. Through the experiments, different setups were designed for the cell seeding and the maintenance of cell culture media flow during live cell imaging:

1. Live cell imaging experiment without flow: The setup preparation was done inside the cell culture hood. Flexible silicon tubes of 0.76 mm (ID) of around 15 cm were cut. Metallic cannulas were introduced in one of the ends of each tube. Each cannula was then inserted in the inlets/outlets of the PDMS chip by manual pressure. In the other extreme of the tubes, we introduced a needle to be able to inject cells and media with a syringe, the whole setup can be appreciated in Figure 23. All the tubes used, were previously cleaned with ethanol and MiliQ. Once the setup was prepared, the channels and microchannels of the chip were filled with media, by introducing cell media through one of the inlets and closing the rest, with a cup, except one from where media could exit, and repeating the procedure for the other inlets/outlets, as is illustrated in Figure 24. After that 1 ml of cell solution was injected with a 1 ml syringe, the rest of the outlets were closed, so, no continuous flow was maintained for this experiment. After injection we left the cells in a spectral confocal laser scanning microscope TCS-SP5 AOBS (Leica) for a live cell imaging video. Depending on the experiment different time-lapses were defined. It will be specified in results section 5.4.3. Jurkat in PDMS microchannels.

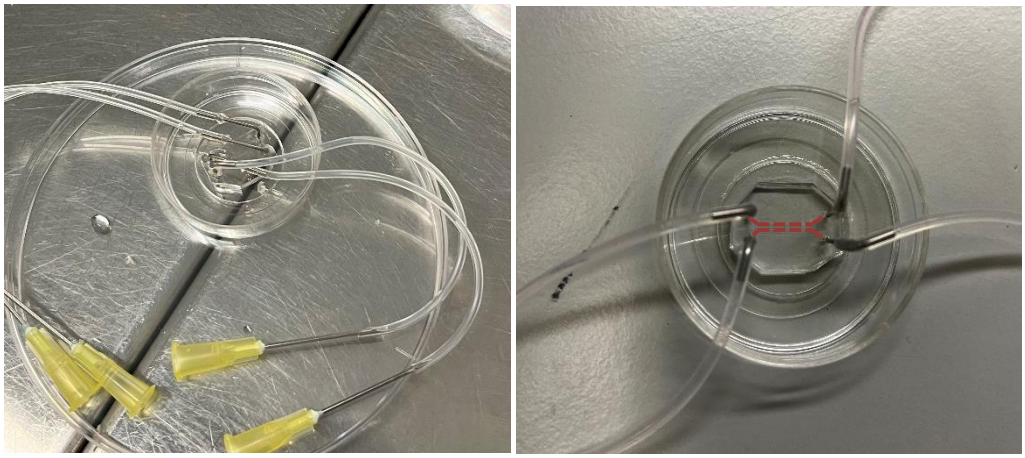

Figure 23: Experimental setup of PDMS microchannels with microfluidic injection approach for Jurkat migration experiments without maintained flow.

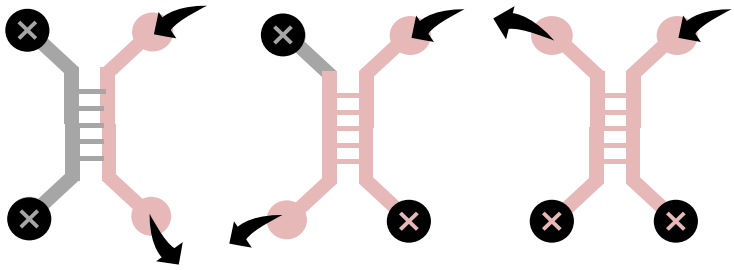

Figure 24: Scheme of the microchannels filling procedure.

2. Live cell imaging experiment with maintained flow: In this case we wanted to maintain a continuous flow of cells or/and media/chemoattractant through the channels during the live cell imaging. To make it possible some changes in the setup were introduced. Some junctions had to be made to make tubes longer. From the previous setup, we took out the needles. For the inlets, we connected the short tubes to longer ones which in turn were connected to the silicon pump tubes, which were placed in a peristaltic pump. From the

other extreme of the pump tubes, another connection was made just to make sure that tubes reached the cells and media reservoirs. Finally for the outlets, a longer tube was connected, and it was left inside the waste reservoir. All connections were done with female - male Luer connectors. Figure 25 shows the final setup. Cells and media were injected at a flow rate of 1 µl/min. And different time-lapses were programmed depending on the specific experiment.

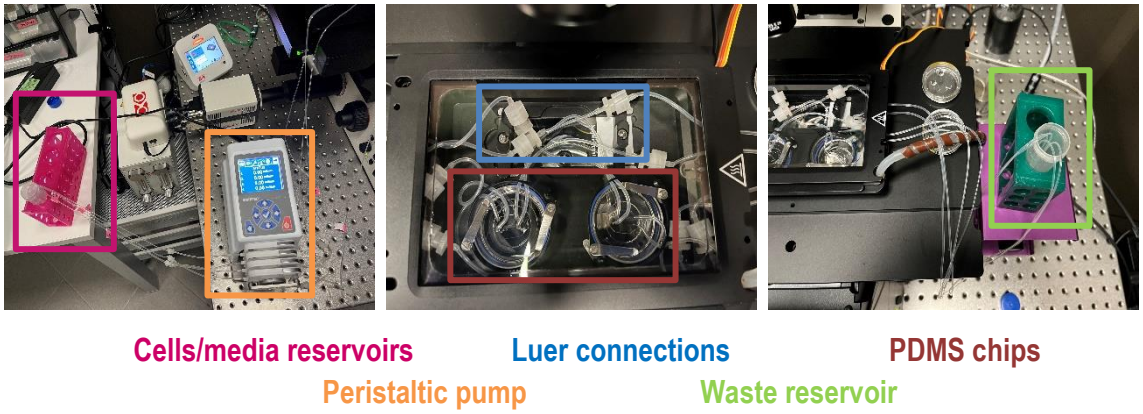

Figure 25: Setup design for live cell imaging experiments with maintained flow.

5. DETAILED ENGINEERING

All the processes detailed above have led us to design, fabricate, arrange, and test a microfluidic device thought to be used in cell migration experiments. The results obtained from the different fabrication methodologies, and from the performed experiments, are being reported and discussed in the following section.

In summary, englobing the different trials and optimization processes, we have developed:

1. A photomask with microchannels designs, to be used in photolithography processes.
2. The SU-8 master, with those designs, to be used as a mold.
3. PDMS and PA microchannels.
4. Confined PDMS and PA microfluidic devices.
5. And finally, different cell experiments have been done to validate the microchannels,
    a. Cell seeding (3T3) on PA hydrogels.
    b. Cell seeding (3T3) on PDMS microchannels.
    c. Cell migration (Jurkat) in PDMS microchannels with static flow.
    d. Cell migration (Jurkat) in PDMS microchannels with continuous flow.

5.1. Obtention of the master with microchannels designs

From the two layered Clewin design of the microchannels, and the delivered photomask, Microfabrication unit of IBEC fabricated the SU-8 master. The two layers were fabricated by two-layer photolithography using different microfabrication approaches since they had different resolution requirements. For the first one, Direct Write Laser was employed and for the second one a photomask was ordered, and UV Photolithography Mask-Aligner technique was used.

5.1.1. Photomask

The acetate photomask of the second layer of the designs, which included the larger channels of the device, and the inlets/outlets, was ordered to JD Photodata, and the received mask was characterized by Microfabrication unit of IBEC.(Figure 26).

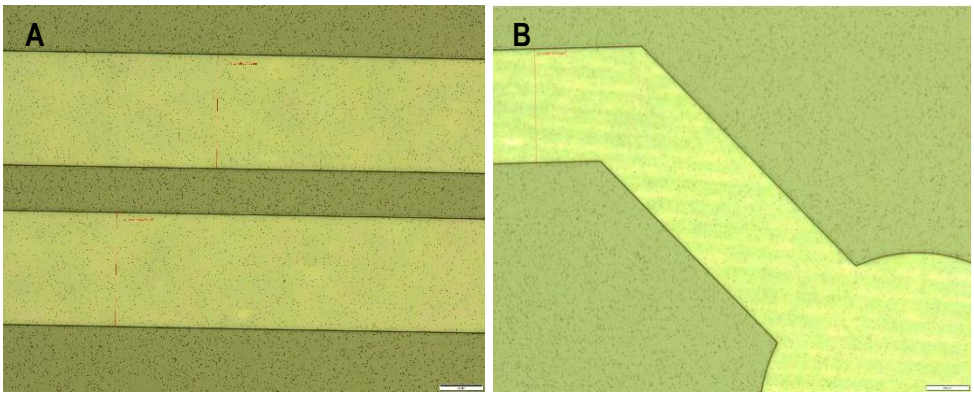

Figure 26: Pictures of provided acetate masks. A) Mask1, 504 µm wide channels, 5x. B) Mask2, 504 µm wide channels, 5x. Scale bar of 200 µm. Source: Microfabrication Unit of IBEC.

5.1.2. SU-8 master

After the different photolithography steps the final master obtained and its characterization can be seen in Figure 27. We were able to obtain the desired mold with all the microchannels designs with a high resolution of features sizes. Channels were straight, without defects, and walls were vertical without any apparent inclination. The molds were developed and prepared to be frequently used. A silanization process was done to ensure the easy detachment of polymerized materials from the master, so that it can be used several times for a longer period of time. It has not broken, neither showed any problem through the whole project and it has been used multiple times per week, so we can confirm that the fabrication process has been successful.

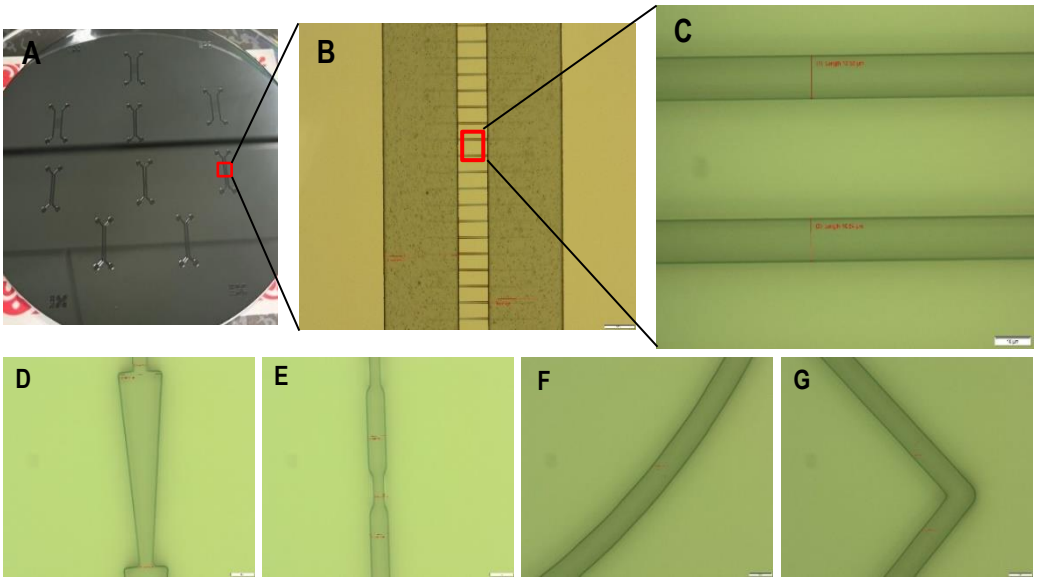

Figure 27: Final SU-8 master obtained. From B-G) Optical microscope images of the master. B) Big channels of 500 µm, 5x magnification. C) Small channels 10,5 µm wide, 100x magnification. D) Small channels 6,7 µm – 19,7 µm wide, 100x magnification. E) Small channels 8,3 µm – 4,9 µm wide, 100x magnification. F) Small channels 10,3 µm wide, 100x magnification. G) Small channels 10,2 µm wide, 100x magnification. Scale bar of 200 µm for B, and scale bar of 10 µm for C-G. Source: Microfabrication unit of IBEC.

5.2. Fabrication of microchannels

Next, we will show the resulting microchannels and their characteristics. As mentioned, we have been working with two different materials for the obtention of microchannels, PDMS and PA.

5.2.1. PDMS microchannels

The fabrication of PDMS microchannels has a simple well stablished protocol and gives very good results. It has been widely used and applied for years in different fields and common problems are already solved. The already explained protocol (4.2.3.1. PDMS microchannels) was carefully followed and PDMS structures of the desired thickness were obtained. Figure 28, shows optical images of the PDMS microchannels where it can be seen that features are well imprinted from the master to the PDMS surface. Therefore, we have not had to deal with important obstacles during this process and we have been able to report favorable outcomes.

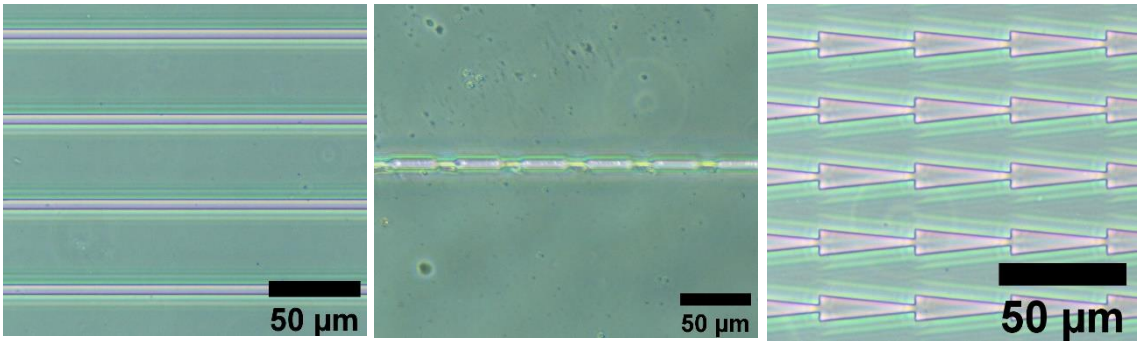

Figure 28: Optical images of different PDMS microchannels, 10x magnification. Scale bar of 50 µm.

5.2.2. PA microchannels

For the fabrication of PA hydrogels two different methods were employed, next we report the obtained hydrogels for both methods and a comparation between them.

5.2.2.1. Replicas fabrication method

The aim of using this method, based on different PDMS replicas to obtain a thin PDMS mold on which polymerization of PA is done, was to avoid demolding problems from the master. Figure 29 shows a summary of the different steps that have been followed. First of all, the PDMS replica was simply obtained, as in the case of PDMS microchannels. The bonding of PDMS to the glass slide was also well acquired, it did not detach during the process. After that, the silanization of the surface and the contra replica obtention, by spin coating a thin layer of PDMS on top, showed good outcomes, the PDMS thin layer could be easily detached from the PDMS mold. Finally, we obtained PDMS pools of 3 mm thickness to polymerize the PA hydrogel inside, using the thin PDMS layer with the microchannels designs as molds. We were able to fabricate PA hydrogels of 3 mm thickness with the microchannels designs imprinted on the surface, as showed in Figure 29E.

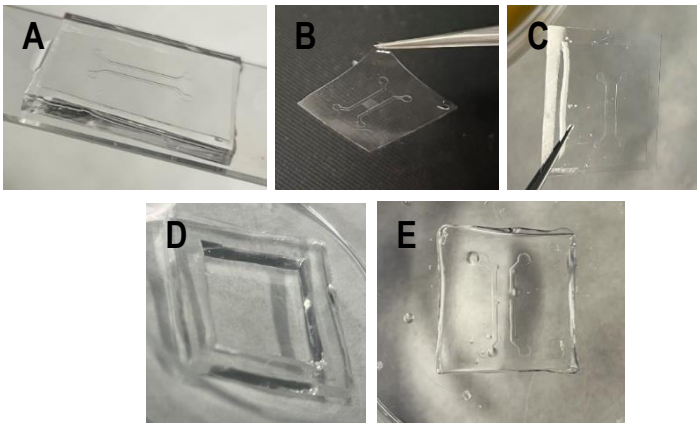

Figure 29: Fabrication of PA hydrogels by PDMS replicas method. From A to C, obtention of the thin PDMS mold. From D to E, PA hydrogel polymerization in PDMS pool.

Nevertheless, the different replicas and steps through the process made the final hydrogel lose resolution. In the different images of Figure 30 can be appreciated how the microchannels are getting less defined and loosing resolution till the point that after 1 day of swelling some of them are even closed. We tried to maintain the most cleaning conditions through the different processes, avoiding any type of waste and the formation of bubbles, but it was difficult to get to the final step without any imperfection or damage. In every step of the fabrication process we were increasing the possible incorporation of bubbles or defects, so the final quality of gels was not good enough. This, at the same time, was compromising further fabrication steps, such as the boning to the flat hydrogel, which required completely flat hydrogels without bubbles. That is why we turned to a different fabrication approach. Moreover, we were measuring the width of microchannels through the different replicas and during the 4 days of swelling and we observed that microchannels of softer gels changed more along the process than those of higher stiffness. This hypothesis was then confirmed by swelling studies for different stiffnesses, in section 5.2.2.3.1. Swelling measurements.

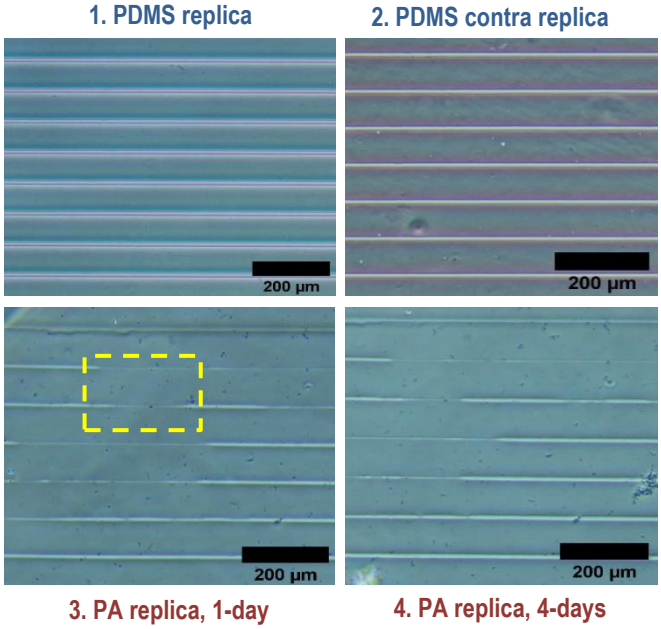

Figure 30: Features resolution through the different replicas of the microchannels.

5.2.2.2. Direct fabrication method

In this case, PA hydrogels were obtained similarly to the PDMS ones. By polymerizing the PA directly on the SU-8 master. This method was not first considered because of the difficulties of demolding the soft hydrogel form the stiffer master surface reported in literature, what could lead to damages in the hydrogel's imprinted features. However, the results obtained were unexpectedly good. As seen in Figure 31, features are better defined than in the previous case, and resolution is well maintained. This fact indicated that the silanization process, carried out during the fabrication of the master, was enough for providing a proper detachment of the hydrogel from the master's surface. Therefore, this was the optimal strategy for acquiring the best quality PA microchannels.

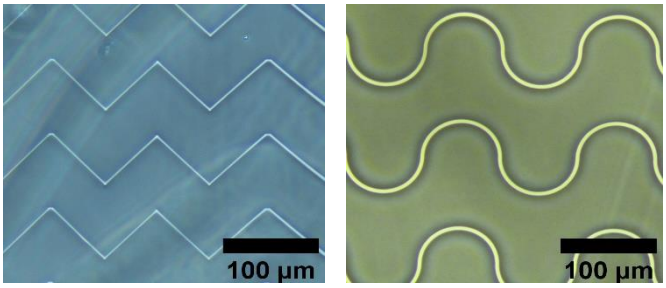

Figure 31: Optical images of the PA microchannels obtained from a direct molding of the master.

5.2.2.3. Characterization of PA microchannels

Additionally, other metrics such as Atomic Force Microscopy (AFM), and swelling measurements, were performed for the characterization of PA microchannels.

5.2.2.3.1. Swelling measurements

Finally, a follow up and study of the hydrogels' swelling was conducted. Hydrogels are polymeric materials which exhibit the ability of incorporating water and retaining a significant fraction of it within their structure without dissolving. Swelling rate is one of the most important technical features of hydrogels. There are different stablished methods to perform swelling ratio experiments, such as Tea-bag method, which is the most conventional method for small amounts of samples [44]. In this case, a simpler method to measure the swelling of hydrogels was followed. We performed the experiment with imprinted hydrogels of the three different studied stiffnesses. The same image of hydrogels, next to a rule, was taken during three days from the fabrication day, and a last image was acquired the 7th day of swelling in the fridge at 4ºC. The images were analyzed with ImageJ. The scale was stablished with the help of the rule and the width of the hydrogel was measured. Figure 32 shows the results obtained. As it can be seen, maximum swelling is commonly reached between day 2-3 of swelling, after these days the gel does not increase, the curve remains constant till day 7th. Furthermore, we can clearly see that softer gels show higher swelling rate. 8kPA hydrogel shows a considerable increase between Day0 and Day2 while 21 kPa hydrogel remains almost stable. This experiment leads us to know that we can use the hydrogels after 2-3 days of fabricating, since we have confirmed that the maximum swelling is then reached. It also allows us to confirm the suspected hypothesis in 5.2.2.1. Replicas fabrication method. Where it was noticed that softer hydrogels showed higher differences in microchannels' width during swelling.

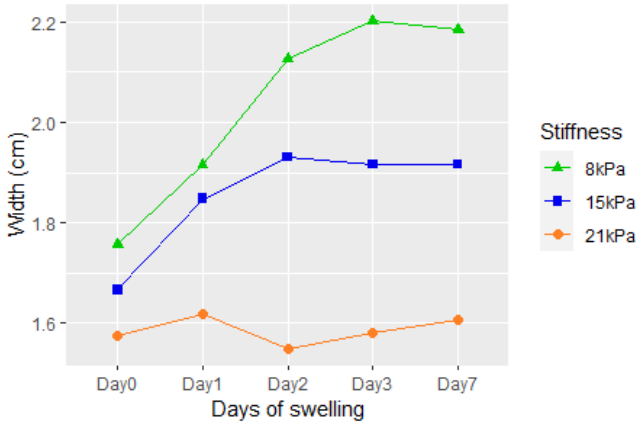

Figure 32: Swelling measurements of hydrogels during 7 days after fabrication.

5.2.2.3.2. Stiffness characterization (AFM)

AFM is not only a tool to image the topography of solid surfaces at high resolution, but it can also be used to measure force vs distance curves. These force curves can inform about different material properties of the surfaces such as stiffness [45]. In the current work, flat PA hydrogels, of the three different stiffnesses studied during the project, were used for AFM measurements after reaching maximum swelling. AFM experiments were performed with a NanoWizard® 4 Bioscience AFM (JPK Instruments) mounted on a Nikon Ti inverted microscope. We used a pyramidal probe with a nominal spring constant of 0.08 N/m. To measure the stiffness (Young's Modulus) of the different gels, force-displacement curves were obtained using contact mode. At least 10 measurements at two different regions were obtained for each gel. Data was processed using JPKSPM Data Processing software. The Young's modulus was obtained by fitting the force-displacement curves with Hertz model. This model relates the applied force (F) by the cantilever tip to the indentation (δ) and the Young's modulus (E) using the equation below, where R is the tip apex radius and ν is the Poisson's ratio, which is assumed to be ~0.5 for soft biological materials. [20]

$$F = \frac{4E}{3(1-\nu^2)} \sqrt[2]{R}\delta^{\frac{3}{2}}$$

From the different values of E obtained for each stiffness we performed the mean and standard deviation, the resulted stiffnesses are reported in Table 5. Moreover, Figure 33 shows an example of the force-displacement curve for each one of the different stiffnesses.

Table 5: Values of the theoretical vs the measured (mean and standard deviation) Young's Modulus of PA hydrogels.

Theoretical Young's Modulus (kPa)	Measured Young's modulus (kPa)
8	8,89 ± 2,12
15	13,27 ± 1,82
21	24,30 ± 6,39

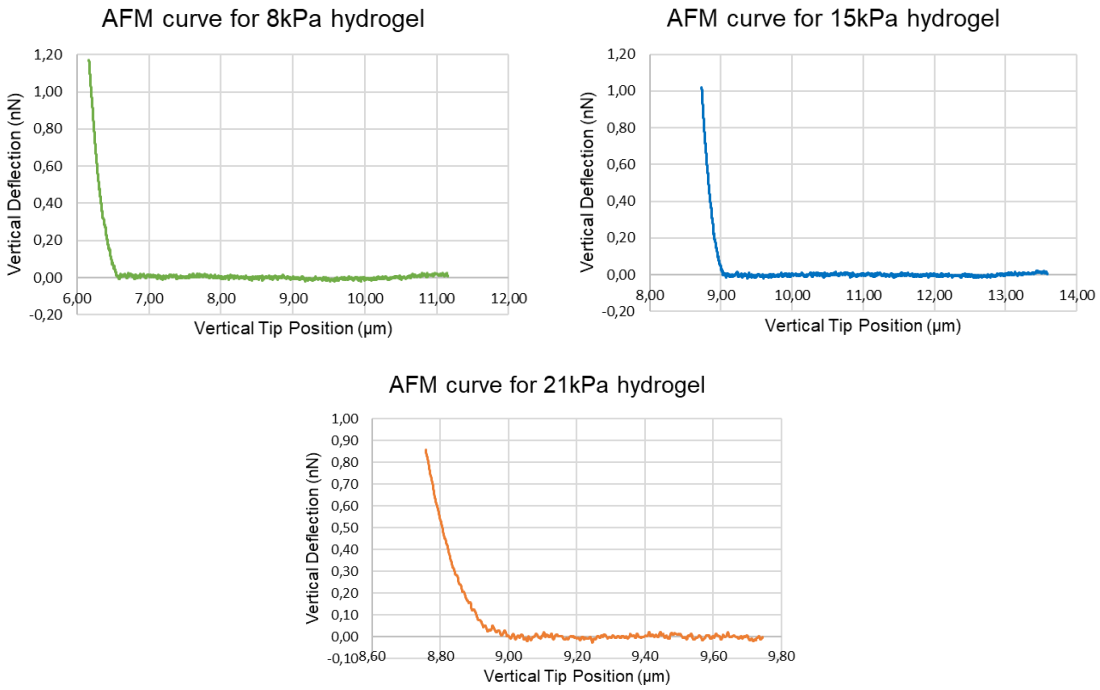

Figure 33: Force-displacement curves for the three different hydrogels' stiffnesses used in the project.

5.3. Bonding and arrangement of confined microchannels

To arrange the final microfluidic device, we bonded the fabricated microchannels to a flat surface obtaining, thus, confined structures. We report next, the obtained results for both cases, first PDMS and second PA microchannels.

5.3.1. Bonding of PDMS channels on glass

The PDMS - glass bonding, performed by plasma activating both surfaces, was successfully achieved. PDMS structures were robustly bonded to the flat glass surface, the final microfluidic chip looked like in Figure 34A. To test the bonding quality and see if channels were functional, some trials with ink were done as showed in Figure 34B, where it can be seen how ink enters the main channels and no leakage is observed outside them. Nevertheless, the bonding process is highly sensitive to the cleaning conditions during manufacturing. Completely clean conditions must be taken and no pressure during bonding must be applied since the microchannels have only 5 µm height and a little pressure can make them bond to the bottom surface and get blocked channels, as happened in Figure 35B. We concluded that the employed protocol was useful and allowed us to obtain chips with functional channels and without leakage.

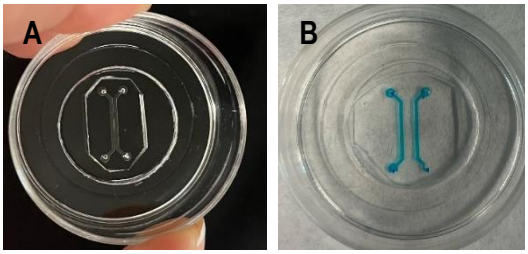

Figure 34: Bonding of PDMS on glass to form confined microchannels. A) Final microfluidic chip. B) Test with ink.

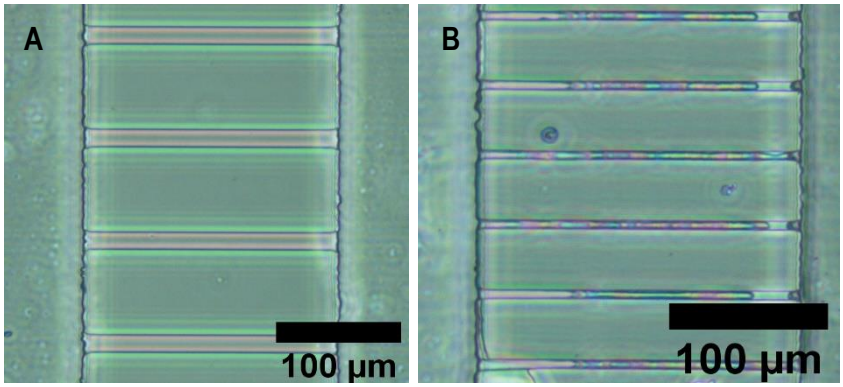

Figure 35: PDMS microchannels after bonding to glass. A) Functional microchannels. B) Blocked microchannels.

5.3.2. Bonding of PA channels

BS3 bonding

For the case of BS3, after tunning some of the aspects through an optimization process, detailed in 4.2.4.2.1. BS3, what we reached was a partial bonding of the PA hydrogel to the flat substrate. As it can be appreciated in Figure 36, after injecting ink through the inlets of the main channels, ink is confined inside the channels in some areas of the device but in others, ink spreads around and under the gel. It means that the bonding has not been uniformly done. Furthermore, after leaving the device with PBS in incubator for some hours it ended up detaching by applying a little pressure on it.

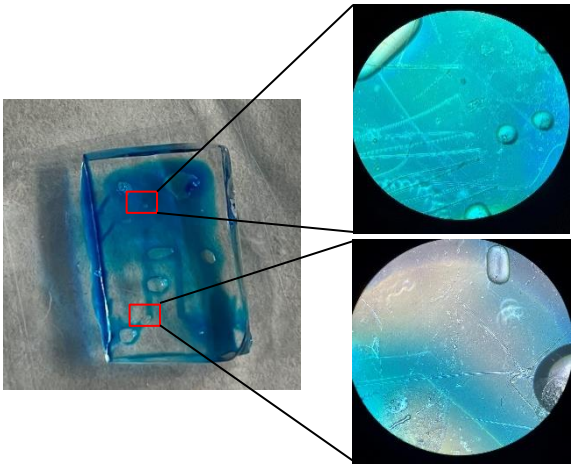

Figure 36: Bonding of PA hydrogels with BS3.

We thought that the bonding was not working at all because of the chemistry of the reaction. BS3 is an NHS ester that reacts with primary amino groups. Several protocols are stablished for NHS coupling with amine groups [46], [47]. However, in this case we are trying to couple NHS ester to the amide groups of the polyacrylamide, and no other previous works have been found reaching that, except from the one from which we are trying to reproduce the protocol. It made us thought that NHS cannot react with amide end of PA. The amide group is less nucleophilic as compared to

the amine group. This is because the electron pair of the amide group is involved in resonance with the neighboring carbonyl group [48], and this may be the reason why the reaction does not occur properly, and gels do not permanently bind.

Diamine bonding

After several failed attempts, we developed a new approach, aiming to fix the chemistry issues detected in the previous methodology. As there were no precedents using this procedure, we had to develop an optimization process to find out which parameters allowed us to obtain better results. This optimization process was based on the same steps as the ones followed in the case of BS3. The idea was to use Sulfo-SANPAH and a diamine molecule to bond both PA hydrogels, as explained in 4.2.4.2.2. Sulfo-SANPAH and diamine. Some of the resulting devices obtained with this method are showed in Figure 37.

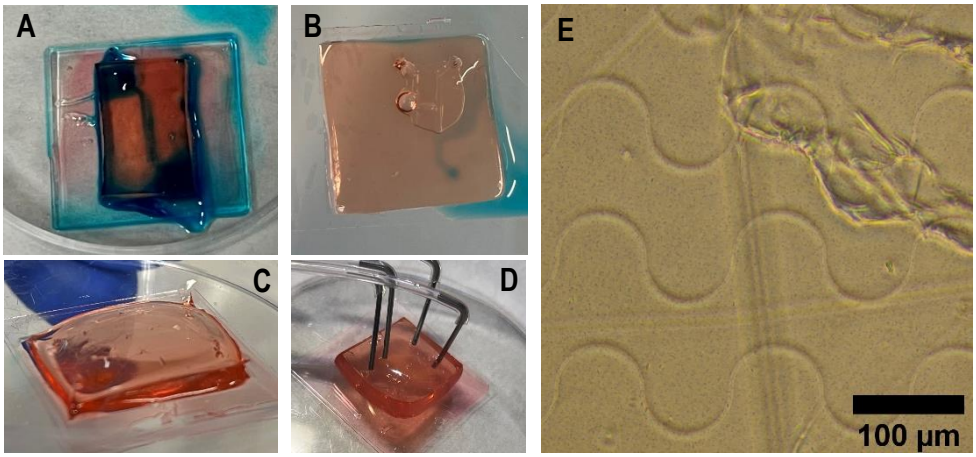

Figure 37: Bonding results with Sulfo-SANPAH plus diamine approach. A and B) Ink seems to enter the main channels but it is also spread through the gel. C) Resulting from adding pressure during bonding. D) Force of cannulas make gels detached. E) After bonding microchannels are still distinguishable.

As it can be seen, no completely successful bonding was achieved neither with this methodology. Nevertheless, microchannels after bonding were still distinguishable (Figure 37E), what in the previous approach (BS3) was not achieved. However, ink was not completely confined inside the microchannels, some leakage was also present. What we noticed was that with this new method, hydrogels seem to be more strongly bonded since they did not detach easily by application of pressure. After 2-3 days in incubator, they were still attached. This could mean that the chemistry of this new process worked better than the previous one.

We tried to improve the method by adding some adjustments to the protocol. We applied pressure during bonding, but it did not succeed (Figure 37C), the gel got crashed and the inlets/outlets were not functional. Furthermore, Figure 37D shows another failed trial where the force of the cannulas, when trying to add ink, made the gel detach form the bottom surface. When adding ink into the channels, you must be very careful because the slightest force applied to the hydrogels can cause them to detach. That's why, for testing, we ended up using the injection pump to be able to better control the pressure made on the hydrogel.

Table 6 recaps the different approaches considered during the optimization process of bonding for both approaches and it highlights those which have showed better results. Although we have not achieved a perfect bonding, many aspects have been modulated and improvements have been made during the process. We have found that the pH of the reactions needs to be adjusted with HEPES buffer to ensure the coupling of molecules to the surface. Which makes sense since both the BS3 and Sulfo-SANPAH reactions are strongly pH-dependent. [40], [41]. We detected that more amount of adhesive solution was not synonym of more attachment. Regarding the time of bonding, better outcomes were obtained if gels were left bonding o/n. Hydrogels were more strongly attached if they were completely dried and adhesive solution was completely adsorbed. Even so, having the hydrogels as long time without PBS, at RT, made them shrink and dehydrate what, at the same time, was affecting the quality of the bonding. Using the hydrogels made by the direct fabrication method reported that microchannels could be well seen and conserved after the bonding what was difficult for the case of replicas fabrication approach.

Table 6: Selected parameters that showed best results during the optimization process of bonding with BS3 and Sulfo-SANPAH + diamine. Adhesive solution corresponds to BS3 solution/diamine solution.

Parameter	Options			
pH	Without HEPES		**With HEPES**	
Amount of adhesive solution	15 µl	24 µl	**50 µl**	75 µl
Time of bonding	20 min	1 h	**o/n**	
Quality of gels	Replicas fabrication method		**Direct fabrication method**	
Pressure during bonding	**Without pressure**		With pressure	
Filling approach	Pipette	Syringe	**Syringe pump**	
Concentration of adhesive solution	Same molar concentration as SS		**50 mg/ml**	

Mechanical bonding

Finally, the last attempt was to make a mechanical bonding, trying to maintain both hydrogels bonded by mechanical pressure but without exerting too much force, what can lead to the blocking of microchannels. The results are reported in Figure 38. This method gave the best results till the moment. From the obtained device with the clips holding the hydrogels bonded, seen in Figure 21 of section 4.2.4.2.3. Mechanical arrangement, we tried to inject ink, but it did not enter through the inlets and channels. We thought that it was maybe due to the pressure exerted to the whole device. Hydrogels were too squashed, and ink could not flow through channels. Then, we removed the clips and hydrogels remained bonded, ink started flowing and as it can be seen in Figure 38A not much ink was spread around the gel. After some minutes there was a little bit of leakage but as appreciated in Figure 38C ink remained in the main channels and the surrounding of the gel

seemed to be quite free of ink. Nevertheless, without any clip holding the device hydrogels ended detaching along time.

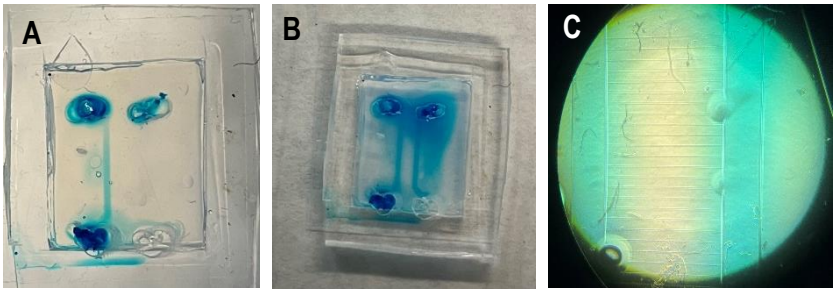

Figure 38: Mechanical bonding results.

5.4. Cell experiments

The final part of the project consisted in testing whether the microfluidic devices developed along the work were compatible with cell experiments, so they were functional and useful for further experiments and research.

5.4.1. 3T3 on PA hydrogel

The first experiment with cells consisted of seeding 3T3 cells on PA hydrogel to see how they behaved when sensing a softer substrate than glass. In Figure 39 we see a clear difference in the shape of cells between the hydrogel and the glass. Cells tend to be more round when spreading on a softer tissue and more elongated when they spread on a harder one like glass. This is in line with previous experiments [49]. To migrate, cells polymerize their cytoskeletons, translocate their body and retract. To do so, they attach by focal adhesion junctions with the substrate and exert forces on it to contract and move. The same force that the cells exert is also exerted by the substrate (in the opposite direction). In the case of glass, because it is harder, the cell exerts force, but the substrate does not move so it stretches and flattens, hence its more elongated shape. In the case of polyacrylamide, when the cell attaches and stretches the substrate, since it is softer, it deforms, and the cell drags it. This is why the cell does not stretch as much and has a more rounded shape [50]. With that we could confirm the effect of softer substrates like hydrogels on cells and it reinforced the advantages of using PA in our device, to mimic the real environment that cells sense *In vivo*.

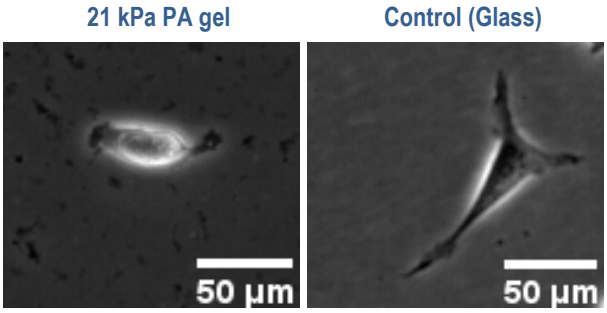

Figure 39: 3T3 cells on PA gel vs glass. Single stack of time-lapse video.

5.4.2. 3T3 in PDMS microchannels

The following experiment aimed to test the microchannels of the fabricated device and to do so, 3T3 cells were seeded through the inlets of the main channels of a PDMS microfluidic chip of 15 µm width microchannels. In Figure 40 we can see a cell inside the microchannel, therefore, the channels of the chip were functional, there was no leakage or detachment from the surface and some of the cells were able to cross the channels, so we can say that the device worked well. Once the set-up was validated, we started experiments with immune cells.

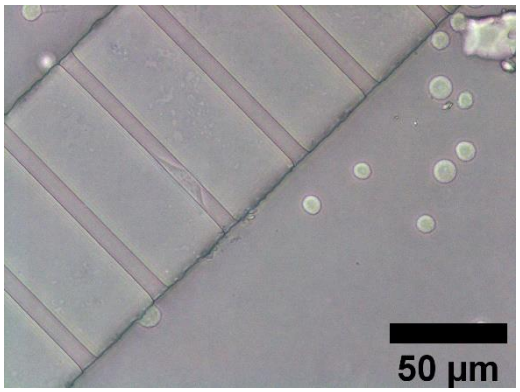

Figure 40: 3T3 cells in PDMS confined microchannels.

5.4.3. Jurkat in PDMS microchannels

The experiments with Jurkat cells aimed to see if these immune cells were able to migrate through channels of 200 µm in length. Previous experiments, performed by other members of the group, showed that these cells can migrate through 5 µm diameter pores over a distance of approximately 10 µm. In addition, in the intravasation and extravasation processes that occur in vivo, cells also have to go through openings of approximately 5 µm. That is why these new experiments have been carried out with 5 µm wide and 200 µm long channels, to see if the cells are still able to migrate.

A we explained in 4.2.5.4. Jurkat on PDMS microchannels section, we designed different setups for this experiment, changing the flow through the channels and the time-lapse parameters of the microscope. Throughout different tests we saw that what worked best was to inject the medium and cells at the beginning of the experiment and not to maintain the flow during the video. Even using the minimum flow rate allowed by the peristaltic pump, the cells moved very fast, and were not able to cross the microchannels. They went from the inlet to the outlet, of the main channel, directly. As far as the video parameters are concerned, we found that taking pictures every minute did not allow to capture the whole path of the cells through the microchannels, because they were crossing them quite fast, so the best way was to make a time lapse of 2 hours maximum and capture the image every 30 seconds.

What we obtained from the different experiments was that cells were able to cross the 200 um microchannels, as seen in Figure 41. But on the other hand, many cells also got stuck in the middle of the channels without moving or creating clumps at the entrance of the channel, blocking it. This last fact is represented in Figure 42.

We can conclude, then, that the dimensions of the channels are optimal to see the migration of the cells, both in length and width. For further experiments we could consider longer channels to see if the cells are still able to migrate longer distances. As for the cell type, we could consider other cells that do not form so many clusters in order to better appreciate the migration process.

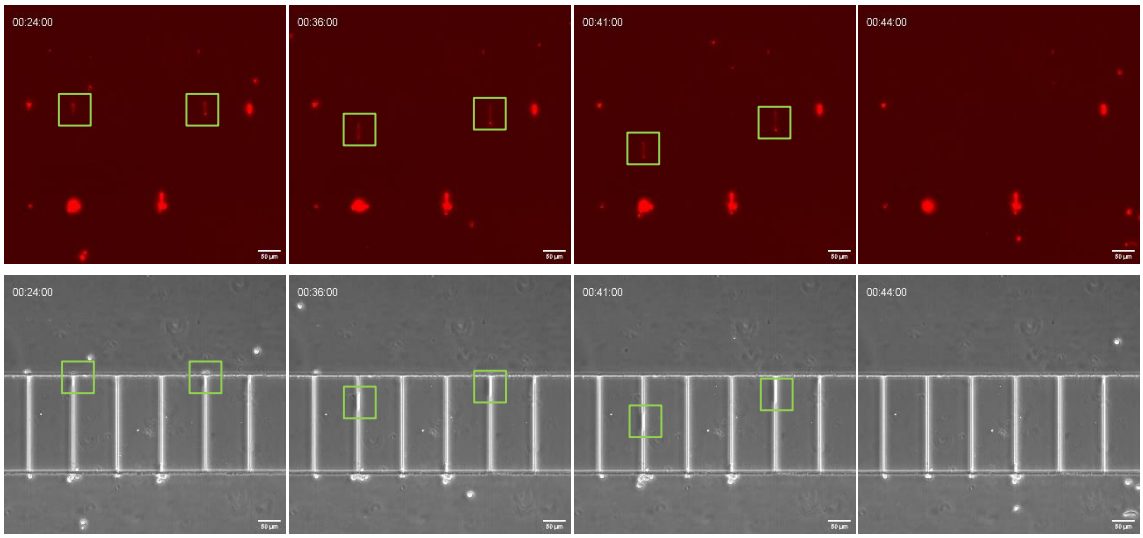

Figure 41: Time lapse of Jurkat cells crossing through 5 µm width microchannels.

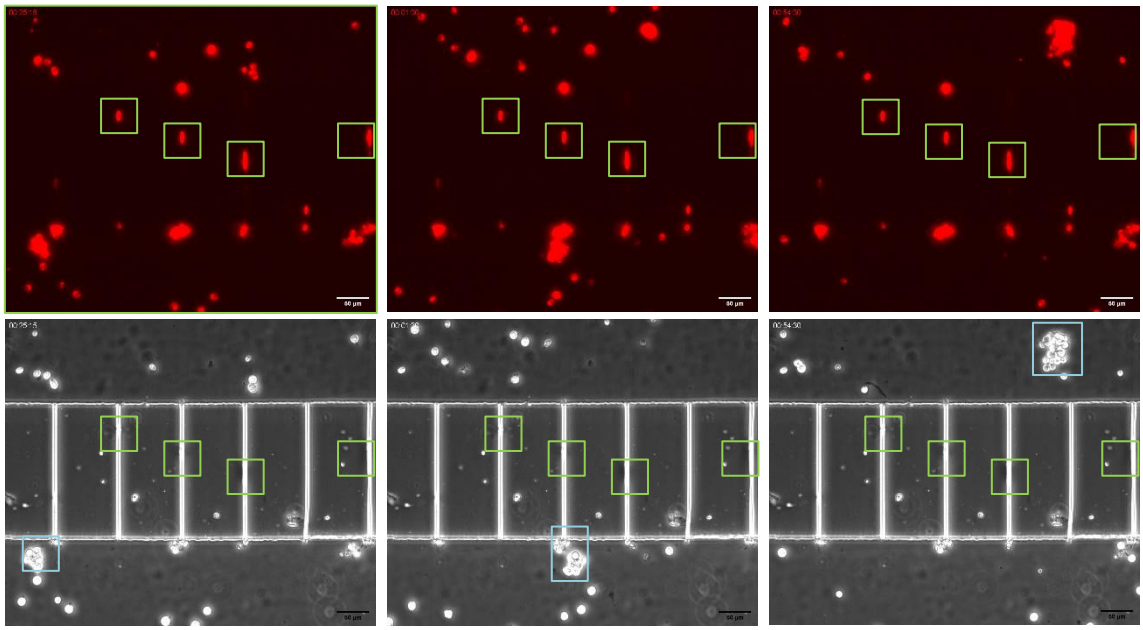

Figure 42: Jurkat cells stagnating in the middle of the microchannels. In green, stagnated cells. In blue, clusters of cells.

6. EXECUTION SCHEDULE

In this section we will make use of different planning tools to define all the activities that must be done, and the time schedule that needs to be accomplished. With that, we will have a temporal view of the project itinerary, and we will be able to do a follow-up of it. The analysis we are applying consists of the Work Breakdown Structure (WBS), and its corresponding activities dictionary, the Project Evaluation and Review Technique (PERT) and lastly the GANTT diagram.

6.1. Work Breakdown Structure (WBS)

Thanks to the WBS we will get a hierarchical decomposition of the different tasks that must be carried out during the project. Based on the most general activities, we will divide them into what are called work packages, which correspond to more specific and easier to manage tasks. It will also help us to define the deliverables we want to obtain and mark, thus, more clear and concrete objectives. In Figure 43 we can see the WBS of the current project. As it shows we have divided the whole project into four principal blocks. They are based on, the management of the project, which will be present throughout the course of the project, the two hardest parts which comprises the design, fabrication, and functionalization of the microfluidic device, and finally a closing phase to validate the final product and analyze the results obtained. Each one of these blocks is subdivided, at the same time, into different specific activities, which are detailed in the WBS's dictionary in the current section.

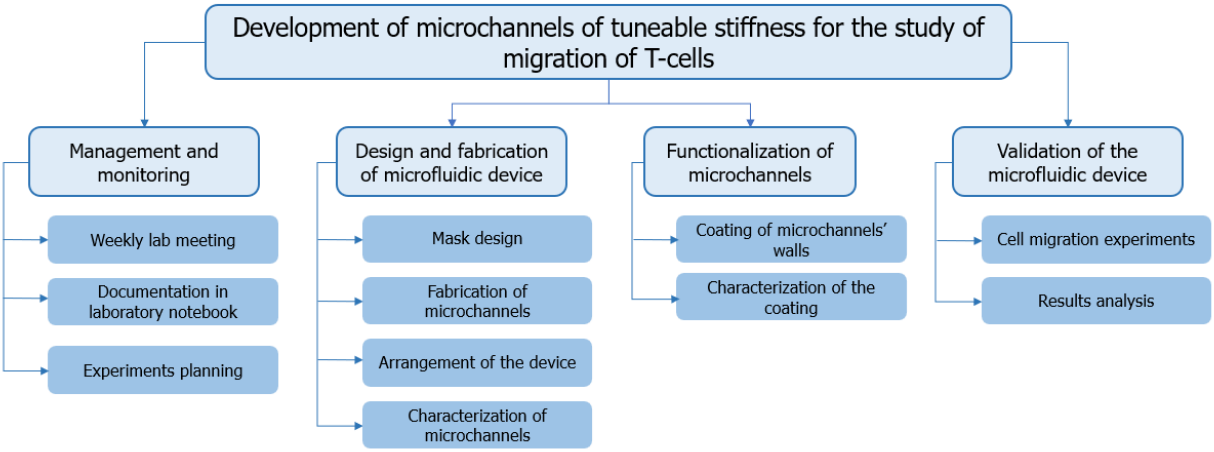

Figure 43: Work Breakdown Structure (WBS) of the project.

Below, is shown the WBS's dictionary, where the different activities are explained. Each activity has an estimated duration time, expressed in days, and the deliverables that must be obtained from it. It has to be said that the duration time is an illustrative estimation, but all the activities will strongly depend on the experiments advances and results, just as on the prolongation of the optimization processes.

1. Management and follow-up

1.1	Experiments planning and start of the project	*Duration*: 10 days
In this first activity we must plan and organize the whole project to have a clear idea of what we want to do and when. We will fix our goals and plan the different experiments and procedures		

that will be done. We must consider that can appear problems during the process so we must adjust the time allowed for each step.
Deliverable: Layout of the project

1.2	Weekly lab meeting	*Duration***:** 300 days
Every week there will be a lab group meeting where all the members of the group expose their advances during the week, it will be useful to discuss problems and doubts about the progress of the project. It will be a way of having a follow-up and control of it.		
Deliverable: Notes of the agreed or solved issues during the meeting.		

1.3	Documentation in laboratory notebook	*Duration***:** 300 days
All the procedures, experiments and tasks performed along the project will be documented in the laboratory notebook, it is important to leave written the exact procedures that have been employed in order to could reproduce them in the future by another person.		
Deliverable: Laboratory notebook with all the processes and experiments carried out.		

2. Design and fabrication of microfluidic device

2.1	Mask design and master obtention	*Duration*: 30 days
In this task we will decide the morphology and dimensions that we want for the channels considering that they must reproduce the in vivo microenvironment. With that we will design the mask for photolithography. This will be performed with CleWin software. Once we have the design finished and verified**,** we can order it from JD Photodata company. It will be sent to the Microfabrication department from IBEC**,** and they will provide us with the final master with microchannels designs ready to be used as mold.		
Deliverables: The 'cif' files with the microchannels designs and the final SU-8 master.		

2.2	Fabrication of microchannels	*Duration*: 68 days
This part includes both the fabrication of PDMS microchannels and PA ones. From the same SU-8 master obtained in the previous activity we can develop PDMS devices with the microchannels designs imprinted. Furthermore, we are interested in developing PA microchannels, so this work package will also comprise the development of a microfabrication protocol, and its optimization process, to obtain PA hydrogels with the microchannels designs imprinted. To be able to arrange the final microfluidic device, in the case of PA microchannels, we will also need to fabricate flat PA hydrogels, so a different protocol to do that must be elaborated in this work, too.		
Deliverables: PDMS structure with microchannels designs imprinted, PA imprinted hydrogel, PA flat hydrogel.		

2.3	Arrangement of the device	*Duration*: 100 days
The aim of this work package is to arrange the final microfluidic device to obtain confined microchannels, using the structures obtained in the previous one. Again, in this activity we will work at the same time with PDMS and PA devices. On one hand, we will bond the PDMS microchannels to a Mattek glass to obtain these confined cavities, on the other hand, we must develop a bonding protocol, and the optimization process it involves, to bond the imprinted PA hydrogel to the flat PA hydrogel to form confined microchannels.		
Deliverables: Final microfluidic device with confined microchannels. Both the PDMS and PA versions.		

2.4	Characterization of microchannels	*Duration*: 20 days
After the fabrication process, we need to validate that the microchannels have the morphology, dimensions and properties aimed, so we need to characterize them. We will measure the dimensions of the microchannels to evaluate the resolution of the fabrication process, with a contrast phase microscope and ImageJ software. We will also measure the stiffness of the PA hydrogels with AFM, and we will finally measure the swelling ratio of the hydrogels.		
Deliverables: Report with graphs and summary of the measures taken.		

3. Functionalization of microchannels

3.1	Coating of microchannels' walls	*Duration*: 6 days
Two different functionally active proteins, an extracellular matrix protein and endothelial cell membrane receptor will be used to coat the walls of the microchannels to functionalize them.		
Deliverables: Coating protocol.		

3.2	Characterization of the coating	*Duration*: 6 days
We need to confirm and verify that the coating has been successful, to do that we will use confocal microscopy.		
Deliverables: Confocal images verifying the coating.		

4. Validation of the microfluidic device

4.1	Cell migration experiments	*Duration*: 60 days
In order to test the device, we will do cell migration experiments with Jurkat cells. It will involve time-lapse experiments and live-cell labeling.		
Deliverables: Videos and images of the experiments.		

4.2	Results analysis	*Duration*: 30 days
Finally, we will analyze the results of the previous experiments and we will conclude if the device has been useful and accomplishes the initial requirements.		
Deliverables: Report of the results and conclusions.		

6.2. PERT-CPM Diagram

In order to obtain the PERT diagram, we have established the preceding activities that must be done before starting each of the different tasks and we have made an estimation of the time needed to carry them out. To acquire a time as close as possible to reality we have used the PERT method which considers that the duration of an activity will follow a beta distribution, it is a probabilistic model and time is defined by Equation 1.

$$\mu_j = \frac{\mu_o + 4\mu_m + \mu_p}{6} \qquad \text{Equation (1)}$$

Where μ_j is the PERT time we will use, μ_o is the most optimistic time, μ_p the most pessimistic time and μ_m the normal time we expect the activity to last. In Table 7 we see the list of activities and their precedents with the calculated times for each of them, represented by T_{PERT}, T_o, T_p and T_{mean}, respectively.

Table 7: Preceding activities and duration time for each activity.

Activity	ID	ID previous activity	T_o	T_{mean}	T_p	T_{PERT}
Experiments planning and start of the project	A	-	5	10	15	10
Mask design	B	A	25	30	35	30
Fabrication of microchannels	C	B	60	68	76	68
Arrangement of the device	D	C	95	100	105	100
Characterization of microchannels	E	C	15	20	25	20
Coating of microchannels' walls	F	D, E	5	6	7	6
Characterization of the coating	G	F	5	6	7	6
Cell migration experiments	H	G	55	60	65	60
Results analysis	I	H	25	30	35	30
Weekly lab meeting	J	A	295	300	305	300
Documentation in laboratory notebook	K	A	295	300	305	300

From Table 7 we can generate the PERT diagram and see the evolution of the tasks along the project. In addition, this tool shows what the critical path is. This one will help us to identify which are the activities in which there should be no delay if we want to finish the project with the minimum possible time.

As we see in the diagram of Figure 44, we had to create a fictitious activity since we had two parallel tasks in one point of the project. In dark blue we see highlighted the two critical paths we have determined, the first corresponds to the supervision of the progress of the project, as expected, since it is the only task that extends during the entire project. The second critical path is conditioned by the two longest works which are the fabrication of microchannels and the arrangement of the device, since this second one comprises a huge optimization task and try and failure process.

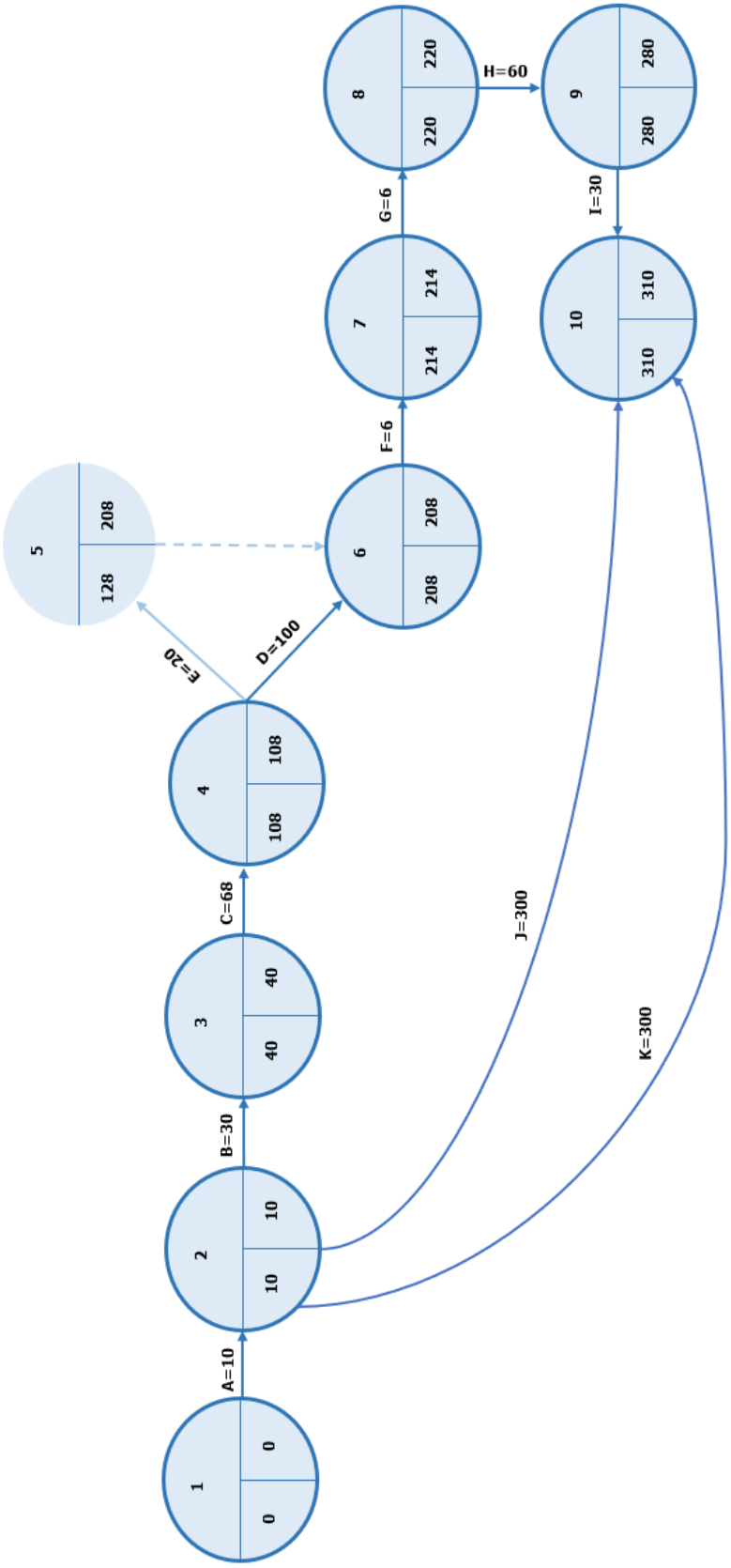

Figure 44: PERT Diagram.

6.3. GANTT Diagram

The GANTT method facilitates the temporal programming of activities and their monitoring. For us it is useful to know the time in which the different tasks must be carried out and to be able to quickly assess whether are on schedule or not. In Figure 45 we see the resulting GANTT diagram of the current project. Orange color marks the critical path, which we have already discussed in the previous section, it tells us about the activities in which there should be no delay.

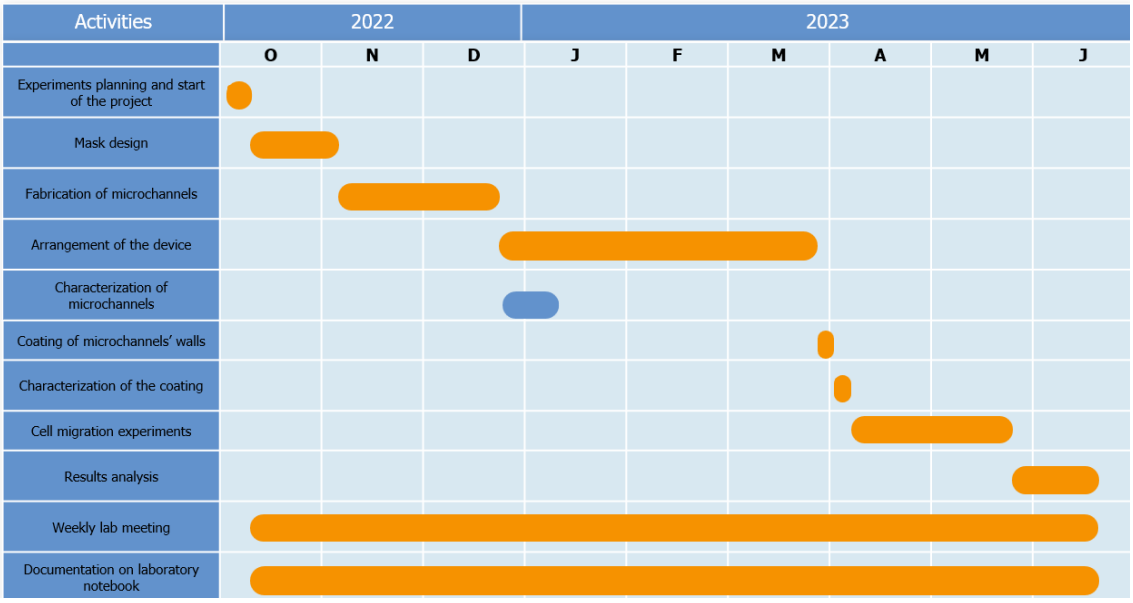

Figure 45: GANTT Diagram.

7. TECHNICAL VIABILITY

To know the technical feasibility of the project we have analyzed the strengths, weaknesses, opportunities, and threats (SWOT) that we face with the current project considering both internal and external aspects. A sum-up of the analysis is seen in Table 8. From it we can conclude that is a challenging project since it aims to develop an almost new approach with very few precedents and stablished protocols. But at the same time, it is a potential technology that can be very well received in many research fields.

Table 8: SWOT analysis of the proposed microfluidic device.

S	INTERNAL **STRENGTHS**
1	Confined microchannels
2	Tunable and physiological stiffness
3	Mimics in vivo environment
4	Biocompatible hydrogel
5	High throughput analysis

W	INTERNAL **WEAKNESSSES**
1	No stablished protocols
2	Bonding approach of hydrogels
3	Not reusable device
4	Easy detaching of hydrogels
5	No ideal cell line to test the device

O	EXTERNAL **OPPORTUNITIES**
1	Great market potential
2	Increasing interest in hydrogel's devices
3	Alternative to animal testing
4	High impact of CRC disease

T	EXTERNAL **THREATS**
1	New technology
2	Lacks product standarization
3	Not ready for industry
4	Strict demans on research fild

8. ECONOMIC VIABILITY

Funding for this project has been provided by IBEC's Biomimetics Systems for cell engineering group. The different equipment and facilities used have been provided by them and by IBEC's core facilities unit. In Table 9 are detailed the different reagents, materials, special equipment, and software employed during the project. An estimation of the total cost of the project has been performed. To the total cost from Table 9, we must add all the fungible material spent during the whole project including, different types of flasks, petri dishes, Eppendorf, Pasteur pipettes, glass coverslips, gloves, syringes, needles, etc. Furthermore, if we suppose a salary of 12,82 €/hour for a Junior Engineer, for the approximately 300 hours spent, the whole cost of the project extents to around 10.700,00 €.

Table 9: Cost of reagents, material, equipment, and software.

	Item (units)	Provider	Unit	Price (€)
LABORATORY REAGENTS	Acrylamide (40%)	Bio-Rad	500 ml	139,00
	N,N-Methylene bisacrylamide (2%)	Bio-Rad	500 ml	121,00
	Ammonium persulfate analytical grade (APS)	Serva	50 g	60,10
	N,N,N',N'-Tetramethylethylenediamine (TEMED)	Sigma	50 ml	66,70
	Phosphate Buffered Saline (PBS)	Sigma	1 l	50,00
	SYLGARD® 184 Silicone Elastomer Kit	Dow Corning	1	173,00
	Bis(sulfosuccinimidyl) suberate (BS3)	Sigma	50 mg	203,00
	HEPES	Life Technologies	100 ml	64,00
	1,6-Diaminohexane	Sigma	5 g	31,60
	Sulfo-SANPAH	Life Technologies	50 mg	375,00
	Dulbecco's Modified Eagle Medium (DMEM)	Corning	500 ml	25,80
	Fetal Bovine Serum (FBS)	Life Technologies	500 ml	175,00
	Pen/Strep	Sigma	100 ml	10,50
	Trypsin-EDTA	Sigma	100 ml	10,50
	Glutaraldehyde 25 wt. % in H2O	Sigma	1 l	1490,00
	(3-Aminopropyl) trimethoxysilane 97 %	Sigma	100 ml	83,20
	Trichloro(1H,1H,2H,2H-perfluorooctyl) silane	Sigma	10 g	110,00
MATERIAL	PMMA shits	Goodfellow	3	10,65
	Mat Tek 35 mm petri dish, 20 mm Microwell	Mat Teck	200	278,77
	Silicon tubes ID 0.76 mm	FREUDENBERG	1	74,00
	Silicon peristaltic pump tubing ID 0.76 mm	ISMATEC	1	91,00
	Luer Fitting, Male Luer 1/16 HB, Natural PVDF	CPC	100	104,55
	Luer Fitting, Female Luer 1/16 HB, Natural PVDF	CPC	100	104,55
	Rapid-Core sampling punches – Ø 0.75mm	Sigma	1	6,93
EQUIPMENT	WS-400A 6TFM/LITE Spin Coater	Laurell Tech	1	*
	Expanded Plasma Cleaner PDC-002-CE (230V)	HARRICK	1	*
	Nikon Eclipse Ts2 inverted microscope	Nikon	1	*
	THUNDER Imager Live Cell & 3D Assay	Leica	1	*
	NanoWizard® 4 Bioscience AFM	JPK Instruments	1	*
	Injection pump (syringe)	WPI	1	1200,00
	Peristaltic pump	ISMATEC	1	1700,00
SOFTWARE	Image J	-	-	Free access
	Clewin5	-	-	*
	JPKSPM Data Processing	-	-	*
	Microsoft Office	-	-	*
	Biorender	-	-	Free access
OTHERS	Photomask	JD Photodata	1	156,00
	Masters	Microfab Unit of IBEC	2	*
TOTAL				**6914,85**

* Equipment provided by IBEC Core Facilities Unit and Biomimetic Systems for Cell Engineering group.

9. REGULATIONS AND LEGAL ASPECTS

The current project does not involve ethical issues. Nevertheless, all the experiments and processes have been done in conformance with national and EU legislation, regulations, and ethical standards, following the basic ethical principles of the EU (2010/C 83/02) [51]. It sets up principles and guidelines for researchers and research institutions within the European Union.

The personal have been working under Directive 2000/54/EC [52]. This EU directive addresses the protection of workers from risks related to exposure to biological agents in the workplace, which can cause infection, allergy, or toxicity. It stablishes minimum health and safety requirements, and it provides basic guidelines for the prevention and control of these risks. Thus, Personal protective equipment (PPE) has been used during the whole development of the project, and all the cell manipulation has been done on a Class II Biosafety cabinet.

For further information, in the case that our device would be launched to the market, other regulations and legislations would be required by research institutions and funding agencies. Good Laboratory Practices (GLP) may be asked for, which involves following standardized protocols, maintaining accurate records, ensuring equipment calibration and other quality control measures. A proper labelling, storage and handling must be done regarding chemical regulations, in the case we included dyes or chemical reagents in our product. And finally, we must inspect some extra regulations such as those stablished by the International Organization for Standardization (ISO). In 2016, a first step towards microfluidic standardization was made with the development of ISO IWA23, which facilitates the uptake of microfluidic devices by making them easier to use, reducing the cost for assembling and enabling plug and play functionality. Also, ISO/TC48/WG3 has been set up to develop microfluidic standards covering metrology for the methodologies and fabrication processes. And more recently, ISO 22916:2022 Microfluidic devices – Interoperability requirements for dimensions, connections and initial device classification was also published. [53]

10. CONCLUSIONS AND FUTURE WORK

The goal of the project was to develop a microfluidic device with narrow channels of controllable size and stiffness. The device aimed to overcome the limitations of the current microfluidic approaches, of supraphysiological stiffnesses, by using PA hydrogels for the fabrication of the microchannels. Which can reach similar Young's Modulus to *In vivo* tissues. With that, the obtained device, is thought to be used to study T-cell migration for colorectal cancer research.

The elaboration of the project has allowed to obtain, with the collaboration of Microfabrication and Characterization Unit of IBEC, two silicon wafers, by a photolithography process. The wafers contain a large variety of microchannel designs of different sizes, ranging from 5 µm to 15 µm width, and, also, different shapes providing several types of constrictions and wavy conformations that can mimic real environments that cells found inside the organisms. The fabricated masters can be used as a mold for PA polymerization or PDMS replica acquisition, for a long time if they are properly conserved. It has been proven that the masters have the correct designs and features well imprinted and with a high resolution, conserving every detail of the original designs. Furthermore, a successful treatment has been done on the surfaces of the masters to guarantee the easy detachment of the polymerized material form it.

We have developed different protocols for the fabrication of microchannels. For the case of PDMS microchannels an already existing protocol has been successfully applied and well-defined narrow channels of PDMS have been easily obtained. On the other hand, for the fabrication of PA microchannels two different protocols have been proposed and progressively improved. One consisted in different PDMS replicas of the mold to obtain a thin PDMS layer to be used as a mold for PA polymerization, and the other was based in a direct polymerization of the PA in the original mold. After several trials we have confirmed that better results and microchannels of higher quality are obtained with the fabrication of microchannels by a direct polymerization of the PA in the silicon wafer molds. Moreover, the swelling capacity and the stiffness of the PA hydrogels have been characterized. We have been able to fabricate PA hydrogels of different stiffnesses from 8 to 21 kPa by simply varying the concentrations of acrylamide and bis-acrylamide of the PA solutions. And it has been showed that softer hydrogels have higher swelling capacity than those with higher Young's Modulus.

Then, we succeeded in the assemble of confined PDMS microchannels to a glass dish by using plasma activation protocols to bond both surfaces, and we were able to obtain a functional microfluidic chip. Even though we could not reach a perfect assembling of PA hydrogels to obtain confined PA microchannels we developed two novel methodologies for bonding two PA hydrogels. A chemical approach was proposed with a previous activation of the surface with Sulfo-SANPAH and using a diamine to get both surfaces attached. An optimization process was carried out to find the best parameters and conditions to reach a permanent bonding but there is still some work to be done. From the other side, a mechanical approach was also designed and performed, and promising results were obtained but, again, some arrangements are needed.

Finally, the PDMS microfluidic chip was tested with cells. Jurkat cells were seeded in the microchannels, and time-lapse videos were obtained to study the migration profile of these T-cell line. We were successful in designing different experimental set ups with different tubing connections to perform experiments with and without maintained flow of cells and/or media/chemoattractant. We could conclude form the experiments that the PDMS chips fabricated were suitable for performing cell migration experiments, no leakage was observed during the testing and the route of cells through the channels could be seen. The dimensions chosen for the designing of microchannels were correct, cells were able to enter the channels and even cross them.

To sum up, we have been able to develop a microfluidic chip of narrow channels that enables the study of T-cells migration. We have failed in incorporating the tunable stiffness in the chip used for cell experiments, but nevertheless, we have got close to obtain confined PA microchannels with our own proposed bonding methodologies. Which have been proved, in the current work, to offer tunable physiological stiffnesses.

For further experiments, we want to test the device with other T-cell lines to see if they have more migrating capacity, as some problems have been observed with Jurkat cells, which tend to form cluster that block the entrance of the channels. Moreover, further effort and dedication will be given to the bonding approach of PA hydrogels since it is a very powerful approach considering the increasing interest in mimicking the characteristics and mechanical properties of *In vivo* tissues.

11. BIBLIOGRAPHY

[1] R. L. Siegel, K. D. Miller, H. E. Fuchs, and A. Jemal, "Cancer Statistics, 2021," *CA Cancer J Clin*, vol. 71, no. 1, pp. 7–33, 2021, doi: 10.3322/caac.21654.

[2] N. Zafari *et al.*, "The role of the tumor microenvironment in colorectal cancer and the potential therapeutic approaches," *J Clin Lab Anal*, vol. 36, no. 8, 2022, doi: 10.1002/jcla.24585.

[3] S. Ben Hamouda and K. Essafi-Benkhadir, "Interplay between Signaling Pathways and Tumor Microenvironment Components: A Paradoxical Role in Colorectal Cancer," *Int J Mol Sci*, vol. 24, no. 6, p. 5600, 2023, doi: 10.3390/ijms24065600.

[4] D. S. Chen and I. Mellman, "Oncology meets immunology: The cancer-immunity cycle," *Immunity*, vol. 39, no. 1, pp. 1–10, 2013, doi: 10.1016/j.immuni.2013.07.012.

[5] W. Polacheck, I. Zervantonakis, and R. Kamm, "Tumor cell migration in complex microenvironments," *Cell Mol Life Sci*, vol. 70, no. 8, pp. 1335–1356, doi: 10.1007/s00018-012-1115-1.Tumor.

[6] K. Konstantopoulos, "Distinct signaling mechanisms regulate migration in unconfined versus confined spaces," vol. 202, no. 5, doi: 10.1083/jcb.201302132.

[7] A. Akbarzadeh *et al.*, "Assessing cell migration in hydrogels : An overview of relevant materials and methods," vol. 18, no. September 2022, 2023, doi: 10.1016/j.mtbio.2022.100537.

[8] W. J. Polacheck, I. K. Zervantonakis, and R. D. Kamm, "Tumor cell migration in complex microenvironments," *Cell Mol Life Sci*, vol. 70, no. 8, pp. 1335–1356, 2013, doi: 10.1007/s00018-012-1115-1.Tumor.

[9] S. BOYDEN, "The chemotactic effect of mixtures of antibody and antigen on polymorphonuclear leucocytes.," *J Exp Med*, vol. 115, no. 3, pp. 453–466, Mar. 1962, doi: 10.1084/jem.115.3.453.

[10] H. J. Wu *et al.*, "Analysis of microglial migration by a micropipette assay," *Nat Protoc*, vol. 9, no. 2, pp. 491–500, 2014, doi: 10.1038/nprot.2014.015.

[11] L. G. Rodriguez, X. Wu, and J.-L. Guan, "Wound-Healing Assay BT - Cell Migration: Developmental Methods and Protocols," J.-L. Guan, Ed., Totowa, NJ: Humana Press, 2005, pp. 23–29. doi: 10.1385/1-59259-860-9:023.

[12] F. Sala, C. Ficorella, R. Osellame, J. A. Käs, and R. Martínez Vázquez, "Microfluidic Lab-on-a-Chip for Studies of Cell Migration under Spatial Confinement," *Biosensors (Basel)*, vol. 12, no. 8, pp. 1–19, 2022, doi: 10.3390/bios12080604.

[13] J. Pihl, J. Sinclair, M. Karlsson, and O. Orwar, "Microfluidics for cell-based assays," *Materials Today*, vol. 8, no. 12, pp. 46–51, 2005, doi: 10.1016/S1369-7021(05)71224-4.

[14] H. Kaji, G. Camci-Unal, R. Langer, and A. Khademhosseini, “Engineering systems for the generation of patterned co-cultures for controlling cell-cell interactions.,” *Biochim Biophys Acta*, vol. 1810, no. 3, pp. 239–250, Mar. 2011, doi: 10.1016/j.bbagen.2010.07.002.

[15] P. Vargas, E. Terriac, A. M. Lennon-Duménil, and M. Piel, “Study of cell migration in microfabricated channels,” *Journal of Visualized Experiments*, no. 84, pp. 1–8, 2014, doi: 10.3791/51099.

[16] Y. Ling *et al.*, “A cell-laden microfluidic hydrogel,” *Lab Chip*, vol. 7, no. 6, pp. 756–762, 2007, doi: 10.1039/b615486g.

[17] Y. Choi, J. E. Kwon, and Y. K. Cho, “Dendritic cell migration is tuned by mechanical stiffness of the confining space,” *Cells*, vol. 10, no. 12, pp. 1–12, 2021, doi: 10.3390/cells10123362.

[18] J. M. Ayuso *et al.*, “Glioblastoma on a microfluidic chip: Generating pseudopalisades and enhancing aggressiveness through blood vessel obstruction events,” *Neuro Oncol*, vol. 19, no. 4, pp. 503–513, 2017, doi: 10.1093/neuonc/now230.

[19] M. Anguiano *et al.*, “The use of mixed collagen-Matrigel matrices of increasing complexity recapitulates the biphasic role of cell adhesion in cancer cell migration: ECM sensing, remodeling and forces at the leading edge of cancer invasion,” *PLoS One*, vol. 15, no. 1, pp. 1–29, 2020, doi: 10.1371/journal.pone.0220019.

[20] S. Chung, R. Sudo, V. Vickerman, I. K. Zervantonakis, and R. D. Kamm, “Microfluidic platforms for studies of angiogenesis, cell migration, and cell-cell interactions: Sixth international bio-fluid mechanics symposium and workshop March 28-30, 2008 Pasadena, California,” *Ann Biomed Eng*, vol. 38, no. 3, pp. 1164–1177, 2010, doi: 10.1007/s10439-010-9899-3.

[21] A. Afthinos *et al.*, “Migration and 3D Traction Force Measurements inside Compliant Microchannels,” *Nano Lett*, vol. 22, no. 18, pp. 7318–7327, 2022, doi: 10.1021/acs.nanolett.2c01261.

[22] “Microfluidics Market,” *Microfluidics Market by Product, Application, Research, Manufacturing, End User and Region -Global Forecast to 2026*, 2021. https://www.marketsandmarkets.com/Market-Reports/microfluidics-market-1305.html?gclid=Cj0KCQjw7PCjBhDwARIsANo7CgkVadL1rMsSr6ztQqlyU6khxw-VbfHRgc6l_FYviSZw48KgTbt7SP8aAjUcEALw_wcB

[23] “Mordor Intelligence,” *MICROFLUIDICS MARKET SIZE & SHARE ANALYSIS - GROWTH TRENDS & FORECASTS (2023 - 2028)*, 2023. https://www.mordorintelligence.com/industry-reports/microfluidics-market?gclid=Cj0KCQjw7PCjBhDwARIsANo7CgnEa8kMSjdBEeiIGyaXK-oyCF_iUi--lPZ7ZrEp12vp7jDZuviGwRwaAo65EALw_wcB

[24] “4D cell Explore better,” *Microchannels Dish*, 2023. https://www.4dcell.com/cell-culture-systems/microchannels/microchannels-dish/

[25] R. L. E. Cano and H. D. E. Lopera, “Introduction to T and B lymphocytes,” Jul. 2013, Accessed: May 07, 2023. [Online]. Available: https://www.ncbi.nlm.nih.gov/books/NBK459471/

[26] L. Wang *et al.*, “Vessel Sampling and Blood Flow Velocity Distribution With Vessel Diameter for Characterizing the Human Bulbar Conjunctival Microvasculature.,” *Eye Contact Lens*, vol. 42, no. 2, pp. 135–140, Mar. 2016, doi: 10.1097/ICL.0000000000000146.

[27] Autodesk, “Autodesk AutoCAD,” 2023. https://www.autodesk.es/products/autocad/overview?term=1-YEAR&tab=subscription

[28] Wieweb, “Wieweb,” *CleWin layout editor*, 2023. https://wieweb.com/site/

[29] Romit Sharma, “TechCrack,” *What is Adobe FreeHand) Uses & Features of Adobre FreeHand*, 2023. https://www.techcrackblog.com/2019/11/adobe-freehand-uses-features.html

[30] S. Prakash and S. Kumar, “Fabrication of microchannels: A review,” *Proc Inst Mech Eng B J Eng Manuf*, vol. 229, no. 8, pp. 1273–1288, 2015, doi: 10.1177/0954405414535581.

[31] A. Srinivasan, J. L. López-Ribot, and A. K. Ramasubramanian, *Microfluidic Applications in Vascular Bioengineering*, no. March 2016. 2010. doi: 10.4018/978-1-61692-004-3.ch001.

[32] Heidelberg Instruments, “Heidelberg Instruments,” *Maskless Laser Lithography*, 2023. https://heidelberg-instruments.com/core-technologies/maskless-laser-lithography/

[33] M. L. Heuzé, O. Collin, E. Terriac, and M. Piel, “Cell Migration in Confinement: A Micro-Channel-Based Assay,” vol. 769, pp. 415–434, 2011, doi: 10.1007/978-1-61779-207-6.

[34] P. Nghe, S. Boulineau, S. Gude, P. Recouvreux, J. S. van Zon, and S. J. Tans, “Microfabricated Polyacrylamide Devices for the Controlled Culture of Growing Cells and Developing Organisms,” *PLoS One*, vol. 8, no. 9, pp. 1–11, 2013, doi: 10.1371/journal.pone.0075537.

[35] D. Ho, J. Zou, B. Zdyrko, K. S. Iyer, and I. Luzinov, “Capillary force lithography: The versatility of this facile approach in developing nanoscale applications,” *Nanoscale*, vol. 7, no. 2, pp. 401–414, 2015, doi: 10.1039/c4nr03565h.

[36] J. Comelles, V. Fernández-majada, N. Berlanga-navarro, and V. Acevedo, “Microfabrication of poly (acrylamide) hydrogels with independently controlled topography and stiffness Microfabrication of poly (acrylamide) hydrogels with independently controlled topography and stiffness,” *Biofabrication*, vol. 12, no. 2, p. 25023, 2020, doi: 10.1088/1758-5090/ab7552.

[37] A. Borók, K. Laboda, and A. Bonyár, “PDMS bonding technologies for microfluidic applications: A review,” *Biosensors (Basel)*, vol. 11, no. 8, 2021, doi: 10.3390/bios11080292.

[38] S. K. Sia and G. M. Whitesides, “Microfluidic devices fabricated in poly(dimethylsiloxane) for biological studies,” *Electrophoresis*, vol. 24, no. 21, pp. 3563–3576, 2003, doi: 10.1002/elps.200305584.

[39] S. Cargou, “Elveflow,” *Soft Lithography: Glass/PDMS bonding*, 2022. https://www.elveflow.com/microfluidic-reviews/soft-lithography-microfabrication/soft-lithography-glass-pdms-bonding/

[40] I. P. Information, “INSTRUCTIONS DSS and BS 3 Crosslinkers,” *Thermo Scientific*, vol. 0747, no. 21555.

[41] M. Weight *et al.*, “INSTRUCTIONS NHS / Nitrophenyl Azide Crosslinkers,” vol. 0747, no. 815.

[42] NIH 3T3 CELL LINE, “NIH 3T3 CELL LINE,” *NIH3T3 Cell Culture*, 2023. https://nih3t3.com/nih3t3-cell-culture/

[43] Wikipedia, “Wikipedia,” *Jurkat cells*, 2023. https://en.wikipedia.org/wiki/Jurkat_cells

[44] K. Zhang, W. Feng, and C. Jin, “Protocol efficiently measuring the swelling rate of hydrogels,” *MethodsX*, vol. 7, no. December 2019, p. 100779, 2020, doi: 10.1016/j.mex.2019.100779.

[45] H. J. Butt, B. Cappella, and M. Kappl, “Force measurements with the atomic force microscope: Technique, interpretation and applications,” *Surf Sci Rep*, vol. 59, no. 1–6, pp. 1–152, 2005, doi: 10.1016/j.surfrep.2005.08.003.

[46] L. L. C. Lumiprobe, “Protocol: NHS Ester Labeling of Amino-Biomolecules,” pp. 1–2, 2010, [Online]. Available: papers3://publication/uuid/7AE29A55-9A6A-4329-93DD-43FF49578BC5

[47] N. J. de Mol and M. J. E. Fischer, “Surface Plasmon Resonance: Methods and Protocols,” *Life Sci*, p. 255, 2010, doi: 10.1007/978-1-60761-670-2.

[48] Janice Gorzynski Smith, *Organic Chemistry*, 5th ed. [Online]. Available: https://www.studysmarter.us/textbooks/chemistry/organic-chemistry-5th/alkyl-halides-and-nucleophilic-substitution/problem-752-question-why-is-the-amine-n-atom-more-nucleophil/

[49] R. Sunyer, A. J. Jin, R. Nossal, and D. L. Sackett, “Fabrication of Hydrogels with Steep Stiffness Gradients for Studying Cell Mechanical Response,” *PLoS One*, vol. 7, no. 10, pp. 1–9, 2012, doi: 10.1371/journal.pone.0046107.

[50] C. M. Kraning-Rush and C. A. Reinhart-King, “Controlling matrix stiffness and topography for the study of tumor cell migration,” *Cell Adh Migr*, vol. 6, no. 3, pp. 274–279, 2012, doi: 10.4161/cam.21076.

[51] P. Office, “Carta Drets Fonamentals UE - Charter of Fundamental Rights of the European Union,” pp. 1–15, 2010, [Online]. Available: papers2://publication/uuid/90029970-285D-4BD0-981D-5E4AA5A7C344

[52] G. Provisions, “Directive 2000 / 54 / EC of the European Parliament and of the Council of 18 September 2000 on the protection of workers from risks related to exposure to biological agents at work (seventh individual directive within the meaning of Article 16 (1) of D,” no. December, 2020.

[53] E. Call, “Establishing metrology standards in microfluidic devices,” pp. 1–3, 2020.